Electrochemical production of sustainable hydrocarbon fuels from CO2 co-electrolysis in eutectic molten melts

Al-Juboori, O., Sher, F., Khalid, U., Niazi, M. B. K. & Chen, G. Z.

Original citation & hyperlink:
Al-Juboori, O, Sher, F, Khalid, U, Niazi, MBK & Chen, GZ 2020, 'Electrochemical production of sustainable hydrocarbon fuels from CO2 co-electrolysis in eutectic molten melts', ACS Sustainable Chemistry & Engineering, vol. 8, no. 34, 14, pp. 12877–12890.
https://dx.doi.org/10.1021/acssuschemeng.0c03314

DOI 10.1021/acssuschemeng.0c03314
ESSN 2168-0485

Publisher: American Chemical Society

Electrochemical production of sustainable hydrocarbon fuels from CO_2 co-electrolysis in eutectic molten melts

Ossama Al-Juboori[1], Farooq Sher[2,*], Ushna Khalid[3], Muhammad Bilal Khan Niazi[4], George Z. Chen[1,5*]

[1]*Department of Chemical and Environmental Engineering, University of Nottingham, University Park, Nottingham NG7 2RD, UK.*

[2]*School of Mechanical, Aerospace and Automotive Engineering, Faculty of Engineering, Environment and Computing, Coventry University, Coventry CV1 5FB, UK*

[3]*Department of Chemistry, University of Agriculture, Faisalabad 38000, Pakistan*

[4]*School of Chemical and Materials Engineering, National University of Sciences and Technology, Islamabad 44000, Pakistan*

[5]*Department of Chemical and Environmental Engineering, Faculty of Science and Engineering, University of Nottingham Ningbo China, University Park, Ningbo 315100, China*

*Corresponding authors:

E-mail address: Farooq.Sher@coventry.ac.uk (F.Sher), George.Chen@nottingham.ac.uk (G.Chen)

Abstract

Due to the heavy reliance of people on the limited fossil fuel as energy resources, global warming has increased to severe levels due to huge CO_2 emission into the atmosphere. To mitigate this situation, a green method is presented here for the conversion of CO_2/H_2O into sustainable hydrocarbon fuels via electrolysis in eutectic molten salts ((KCl-LiCl; 41:59 mol%), (LiOH-NaOH; 27:73 mol%), (KOH-NaOH; 50:50 mol%), (Li_2CO_3-Na_2CO_3-K_2CO_3; 43.5:31.5:25 mol%)) at the conditions of 1.5–2 V and 225–475 ^oC depending upon molten electrolyte used. Gas chromatography (GC) and GC-MS techniques were employed to analyse the content of gaseous products. The electrolysis results in hydrocarbon production with maximum 59.30, 87.70 and 99% faraday efficiency in case of molten chloride, molten hydroxide and molten carbonate electrolytes under the temperature of 375, 275 and 425 ^oC

respectively. The Gas chromatography (GC) with FID and TCD detectors and GC-MS analysis confirmed that the H_2 and CH_4 were the main products in case of molten chlorides and hydroxides at 2 V applied voltage while longer hydrocarbons (>C_1) were obtained only in molten carbonates at 1.5 V. Through this manner, electricity is transformed into chemical energy. The heating values obtained from the produced hydrocarbon fuels are satisfactory for further application. The practice of molten salts could be a promising and encouraging technology for further fundamental investigation for sustainable hydrocarbon fuel formation with more product concentrations due to its fast-electrolytic conversion rate without the use of catalyst.

Keywords: Sustainable fuels; Molten salts; Co-electrolysis; Hydrocarbon fuels, Electrolyte mixture; CH_4 and H_2 production.

Introduction

Over the past few decades, two major issues have captured the attention of scientists and policymakers: global warming due to the increasing levels of carbon dioxide gas (CO_2) in the atmosphere, and the rapid depletion of fossil fuels as an energy resource. To tackle these complications, two solutions were proposed [1, 2]. The first solution is the use of renewable energy resources such as wind, solar, nuclear or geothermal energy to minimize the greenhouse gases' emission. While the second solution is the consumption of CO_2 to remove its excessive concentration from the atmosphere and to enhance energy resources by converting it into hydrocarbon fuels [3, 4]. Renewable energy resources do not involve CO_2 sequestration [5]. So to tackle CO_2 emissions [6], it was considered preferable to introduce some of the renewable energy resources into an existing energy infrastructure as a "drop-in" form of energy. Examples of this can include the synthesis of fuels or fertilizers from CO_2 or biomass [7, 8].

At present, technologies studied for transforming CO_2 include chemical, photochemical, electrochemical [9] and biological transformation into hydrocarbons [10], nano-carbons [11], nanotubes, and alcohols (methanol and ethanol) [4]. However, these low-value hydrocarbons and methanol produced at low system efficiencies undermine the rationale of this approach. The process of CO_2 and water co-electrolysis at low temperatures (<100 ºC) in aqueous media to convert CO_2 to CO or hydrocarbon species was employed by scientists [12, 13]. However, a suitable catalyst is necessary for this conversion process in order to reduce energy consumption, improve reaction kinetics and product selectivity [14, 15]. Which results in low hydrocarbon gas production due to the poor solubility of CO_2 in aqueous media and the proximity of the electro-reduction potential of both water and CO_2. Consequently, limiting the future use of this process.

Using high temperature electrolysis between 800 and 1000 ºC, provided both thermodynamic and kinetic advantages throughout the reduction of both CO_2 and H_2O. One thing to mention here is that this process not only converts CO_2 into hydrocarbons but also able to produce hydrogen fuel by the splitting of water. Hydrogen gas has been produced by various methods such as plasma arc decomposition, bio-photolysis, coal gasification, dark fermentation, artificial photosynthesis, electrolysis etc [16]. But the electrolysis has proved successful among all due to the good energy efficiency and low cost [17]. Two types of cells were used for high temperature electrolysis: those with solid oxide electrolytes and with molten salts [18, 19].

Recently the use of solid oxide electrolysis cells (SOEC) has gained much interest in the preparation of syngas ($CO+H_2$), hydrogen or methane gas from the CO_2-H_2O co-electrolysis [20, 21]. However, certain limitations such as low production rate, specific electrode materials,

higher production costs, lower durability and high energy utilization, became the reason for their rejection on industrial scale implementation [22]. Molten salts exhibit the same chemistry regarding CO_2 and H_2O reduction as in SOEC except that CO_2 can be also reduced to carbon [23] in addition to carbon monoxide depending on the operating conditions. Which can thereby affect the products. Deposited carbon on cathode can facilitate the formation of different kinds of hydrocarbons (rather than CO) in case of molten salt electrolysis. Because as soon as the fresh carbon deposit on cathode it reacts immediately with hydrogen gas produced via water reduction on the metal cathode surface itself, resulting in the formation of hydrocarbons [24].

Molten salts are preferred over solid oxides regarding CO_2-H_2O co-electrolysis for a variety of reasons. Besides a wide electrochemical window, high electric conductivity, relatively low cost, reactivity with CO_2 and no need of specific electrode materials (Ni-YSZ, $La_{1-x}Sr_xMnO_3$/YSZ) make them suitable candidates for this process. Moreover, the possibility of carbon or CO hydrogenation after electrolysis in molten salts is much more significant [25, 26]. Molten salts with some limitations such as slight corrosion activity particularly at high temperature and relatively high energy utilisation to maintain the heat for molten salt to avoid the solidification [27], can still be employed to produce hydrocarbon gas or liquid fuels [28, 29]. Recently carbon nanotubes (CN) and carbon nano-fibrils (CNF) have been produced by using molten chlorides [30], molten carbonates [31] and molten hydroxides with sufficient conditions of electrolyte combinations, electrode materials, current and temperature etc [32-34].

Moreover, recent investigations also showed the production of syngas (CO, H_2) and methane by employing molten carbonates (Li_2CO_3-Na_2CO_3-K_2CO_3) [24, 35]. There is lack of literature of finding suitable molten salt electrolyte for the co-electrolysis of CO_2 and H_2O to produce hydrocarbon fuels (CH_4 or longer chain). To the best of our knowledge, molten hydroxides

((LiOH-NaOH; 27:73 mol%), (KOH-NaOH; 50:50 mol %)) and molten chlorides (LiCl-KCl; 58.5:41.5 mol%) have never been evaluated for CO_2 to methane conversion. And molten carbonates (Li_2CO_3-Na_2CO_3-K_2CO_3; 43.5:31.5:25 mol%) have never been studied particularly for higher hydrocarbon fuel (>C_1) production via CO_2-H_2O co-electrolysis. So this study aims to fill the research gap in the literature.

This study systematically investigates the hydrocarbon fuel production by employing CO_2-H_2O co-electrolysis by using different types of molten electrolytes: molten chloride (LiCl-KCl; 58.5:41.5 mol%), molten hydroxide ((LiOH-NaOH; 27:73 mol%), (KOH-NaOH; 50:50 mol%)) and molten carbonate (Li_2CO_3-Na_2CO_3-K_2CO_3; 43.5:31.5:25 mol%) at variable conditions of temperature and voltage depending upon the molten salt. Two feed gas insertion methods are also employed; gas flowing over the electrolyte surface (GFOE) and gas flowing inside the electrolyte (GFIE). The effect of different variables including; faradays efficiency, energy consumption and heating values at variable conditions of temperature and voltage are studied. Moreover, the product formation by electrolysis is confirmed by GC (using FID and TCD detectors) and GC-MS.

Experimental

Chemicals

Lithium carbonate **(**Li_2CO_3; ≥99%**),** sodium carbonate (Na_2CO_3; ≥99.5%), potassium carbonate (K_2CO_3; ≥99%**),** lithium chloride (LiCl; 99%), potassium chloride (KCl; >99.9%), lithium hydroxide (LiOH; ≥98% powder), sodium hydroxide (NaOH; ≥98% pellets), and potassium hydroxide (KOH; 90% flakes) were purchased from Sigma-Aldrich, USA. Carbon dioxide (CO_2; 99.99%) and argon (Ar; 99.99%) were procured from Air products. Labovac 10 mineral oil was got from Jencons.

Electrochemical performance measurement

The electrochemical processes were performed by using four combinations of molten salts as electrolytes. The key point of choosing these combinations of molten salts is due to their low melting points and the ability to work at operating temperatures, as low as possible, keeping them in liquid state to enable electrolysis and promote hydrocarbon formation. The composition selection of binary mixtures (LiCl-KCl, LiOH-NaOH and KOH-NaOH) was done on the basis of thermodynamic phase diagrams as illustrated from the **Fig. S1**. The ternary phase diagram (**Fig. S2**) is clearly indicating the composition selection of ternary molten salt mixture (Li_2CO_3-Na_2CO_3-K_2CO_3). Therefore, the salts selected for this study along with their compositions are: LiCl-KCl (58.5: 41.5 mol%), LiOH-NaOH (27: 73 mol%), KOH-NaOH (50: 50 mol%) and Li_2CO_3-Na_2CO_3-K_2CO_3 (43.5: 31.5: 25 mol%), having eutectic melting temperatures of 361, 218, 170 and 397 ^oC respectively. The electrolyte salts were dried in an oven at 200 ^oC for 4 h at atmospheric pressure before their mixing to remove any sort of water impurity.

Then electrolytes were poured into a crucible present inside a corrosion resistant electrolyser's retort. Which was built in house with a flange type cover using the 316-grade stainless steel to shape the reactor to provide and control the environment needed for the molten salt electrolysis. The dimensions of the retort were 130 mm internal diameter, 7.5 mm wall thickness and 800 mm vertical length. On the flange cover, there were some holes drilled for the insertion of ceramic tubes (for anode and cathode gas collection), observation purposes and sealing. The retort was inserted centrally in the furnace. In the retort, a stainless-steel stand was placed and a refractory brick mounted on it and above its alumina crucible containing pre-melted molten salt electrolyte (about 100 g) was placed. The two-electrode mode experimental set-up used here is a continuous system with small scale for electrolysis and hydrocarbon production. The

electrolysis is conducted by using titanium metal (Purity: 99.99%, Good fellow Cambridge Ltd) as cathode and graphite (Purity: 99.99%, Advent Research Materials) as anode [36, 37].

A small rate of gas (CO_2; 48.4%, + H_2O; 3.2% + Ar; 48.4%) flows continuously inside the reactor where hydrocarbons and O_2 gases are produced inside the molten salts on the cathode and anode surfaces respectively during the electrolysis. And the products are collected at different time intervals. This process is done by employing the Agilent E3633A 20A/10V Auto-Ranging DC Power Supply and a laptop with an EXCEL add-in to collect the instrumentation data. Two electrode tube gas outlets were present, each connected to another Dreschel bottle containing the mineral oil to observe the outlet gases produced and reduce electrolyte contamination. Gas product samples were collected using a tedler 1 L (SKC Ltd.) gas bag via a connection from the cathodic gas tube. The electrolyser setup is a modified form of previously used setups [38].The schematic representation of experimental setup is shown in **Fig. 1**

To avoid their mixing, the argon gas was used which pushed the gaseous products into their respective bags. Moreover, the study is carried out with two modes of feed gas insertion inside the reactor for each electrolyte; gas flowing over the electrolyte surface (GFOE) and gas flowing inside the electrolyte (GFIE) for the comparison of hydrocarbon production in both cases. The first method (GFOE) has been used to minimize the chances of solid material's production (carbon, carbon nanotubes, graphene, carbonates solidification) [34, 39] and to produce gaseous hydrocarbon products preferably. The current efficiency was calculated from the **Eqs. (1-2)**:

$$\text{Current efficiency} = \frac{Q_x}{Q_T} \times 100 \quad (1)$$

$$Q_x = nNF \quad (2)$$

where Q_x is the charge required for the amount of individual product produced, n is the number of electrons required, F is the charge of one electron which equals 96485 col and Q_T is the total charge calculated from the area under the current vs time curve.

Characterization

Gas chromatography (GC) (PerkinElmer Clarus 580) was used to analyse the gas products generated from electrolysis with detectors such as the flame ionization detector (FID) and thermal conductivity detector (TCD) for organic compound analysis and a wide range of both organic and inorganic species respectively. The gaseous product species in the sample were identified and quantified by comparison with two different calibration gas standards. The first one is the permanent gas standard with composition of H_2 10%, CO_2 10% and CO 40% for TCD detector and the second standard calibration gas contains ethene (C_2H_4) 0.2%, propylene (C_3H_6) 0.2%, 1-butene (C_4H_8) 0.2%, 1-pentene (C_5H_{10}) 0.2%, methane (CH_4) 20%, ethane (C_2H_6) 10%, propane (C_3H_8) 5%, n-butane (C_4H_{10}) 2%, n-pentane (C_5H_{12}) 1% for the FID detector.

The remaining composition of both gas standards was balanced with helium gas. The GC graphs for different calibration gas standards are shown in **Fig. 2** for the comparison of electrolysis gaseous products. Furthermore, the samples were analysed by a different sophisticated GC instrument (Agilent 7890B) attached with a mass spectrometer (JEOL AccuTOF GCX) for longer chain hydrocarbons detection. Gas detecting tubes from GASTEC (ai-cbss Ltd.) were used to analyse the feed gas compositions for CO_2 and H_2O contents. The feed gas composition with CO_2 (48.4%) + H_2O (3.2%) + Ar (48.4%) was kept same for all the experiments. GASTEC 2HH is characterised to detect the higher contents of CO_2 from 5 to 40% of the feed gas, with the change in colour from orange to yellow.

The GASTEC30 tube can analyse water content in the range of 0–18 mg/L, and it contains $Mg(ClO_4)_2$. However, the colour here will change from yellowish green to purple. After the analysis of cathodic gas sample, the concentration of each gas compound (M_{gas}) was calculated as followed by the **Eq. (3)**:

$$M_{gas} = \frac{A_{gas}/\overline{F}_i}{A_s/M_s} \quad (3)$$

where M_{gas} is the concentration (%) of individual gas in the sample. M_s is the concentration (%) of the specific standard gas in the sample. A_{gas} is the area under the peak resulting from the FID analysis for the individual gas (C_2-C_5) in the sample. A_s is the area under the peak resulting from the analysis of the specific gas standard (CH_4). $\overline{F_1}$ is the response factor for each gas.

Results and discussion

Optimization of electrolytes

The selection of the molten salt is done based on the ability to generate hydrocarbon fuels from the co-reduction of CO_2 and H_2O (**Eq. (4)**). The combination of a hydrocarbon molecule starts ideally from the two known element sources: carbon (C) and hydrogen (H). Both of these elements can be effectively formed from electrochemical conversion via an appropriate molten salt.

$$xCO_2 + y/2H_2O \rightarrow C_xH_y + (x + y/4)O_2 \quad (4)$$

Generally, the presence of moisture with CO_2 gas in molten salt experiments is the basis for generating H_2 and CH_4 during electrolysis in most cases and provide feasibility to the reactions [40, 41].

Molten chloride electrolyte

The attractive characteristic in the molten chloride case is the probability of producing CO or C directly from CO_2 reduction in the presence or absence of a carbonate ion [41]. Carbonate ions (if added externally) are used as an important additive to molten chlorides to provide the oxide ions required for performing CO_2 reduction [42, 43]. For absorbing more CO_2 gas into the molten salt leading to increase in product yield from electrolysis, the addition of oxides or carbonate salts into the molten chloride is considered preferable. But one drawback exhibited by this process was the increase in applied voltage and working temperature of resulting molten salt mixture. Which is not the favourable condition for hydrocarbon production [44]. So to tackle this problem, molten chloride electrolyte is used in this study for hydrocarbon production without any externally added oxide or carbonate salts. In the absence of H_2O and carbonate ions, the reduction of CO_2 to carbon or CO can be done in several steps as seen from the **Eqs. (5-7)** [45].

$$CO_2 + 2e^- \rightarrow CO_2^{2-} \quad (5)$$

$$CO_2^{2-} \rightarrow CO + O^{2-} \quad (6)$$

$$CO + 2e^- \rightarrow C + O^{2-} \quad (7)$$

In the presence of steam beside CO_2 in the feed gas, the reduction of CO_2 becomes more feasible as CO_2 can react with hydroxide ions released from the primary reduction of H_2O through to the one-electron transfer reaction. Moreover, carbonate ions can be generated even from molten chloride through the reaction of CO_2 with oxide ions emitted in turn after the direct reduction of H_2O to H_2 gas (**Eq. (9)**) [46]. The carbonate ions can then be electro-reduced in turn to carbon or CO and produce hydrocarbon by reacting with H_2. The overall reaction occurring at electrodes can be summarised from the **Eqs. (11-13).**

$$H_2O + e^- \rightarrow H + OH^- \quad (8)$$

$$H_2O + 2e^- \rightarrow H_2 + O^{2-} \quad (9)$$

$$CO_2 + OH^- \rightarrow CO_3^{2-} + H_2O \quad (10)$$

Overall reaction

At cathode: $$CO_3^{2-} + 4OH^- + 8e^- \rightarrow CH_4 + 7O^{2-} \quad (11)$$

$$2OH^- + 2e^- \rightarrow H_2 + 2O^{2-} \quad (12)$$

At anode: $$2O^{2-} \rightarrow O_2 + 2e^- \quad (13)$$

It is preferable to perform CO_2-H_2O co-electrolysis at temperatures even lower than the 400 ^oC to form the hydrocarbons feasibly. For that purpose, electrolysis was performed at 375 ^oC and 2V using molten chloride (LiCl-KCl; 41: 59 mol%) with two modes of gas insertion: GFOE and GFIE. The feed gas in GFOE mode containing H_2O, CO_2 and Ar, was kept flowing over the LiCl-KCl (41: 59 mol%) at 1.3 bar. The feed gas pressure was applied slightly over 1 atm to increase CO_2 activity and thus the opportunity of improving reduction inside the molten chloride.

The same experiment was performed at the above conditions using a feed gas containing H_2O with no CO_2. Both experiments in GFOE mode are performed to see the solubility of CO_2 and thus its activity inside molten chlorides. Carrying out electrolysis at 2 V and 375 ^oC, it can be seen from **Fig. 3** that there is a small difference between the two current curves resulting from electrolysis in both cases. However, the current was still relatively high in both cases and gradually decreased with time. The decline in current can be imputed generally to the drop of oxidant concentration (H_2O, CO_2) that is reduced on the cathode surface due to the accumulation of new products (such as H or H_2 bubbles) as there is no renewal action on the cathode surface during electrolysis. Also, it can be noted that the current was slightly higher in the case where CO_2 gas was absent basically due to the obstruction of CO_2 gas against H_2O

reduction on the electrode, particularly at high pressures through the possible reduction of CO_2 to CO_2^{2-} (**Eq. (5)**).

Despite some spikes noticed in the red curve in **Fig. 3**, it can be seen that the drop of the curves in both cases was quite the same confirming the weak effect of CO_2 inside the molten chloride in GFOE mode. So due to CO_2 weak effect, the hydrocarbon could not be produced in this case (GFOE mode). The GFIE mode of gas feed introduction was chosen as an appropriate way to increase CO_2 concentration and solubility (and reactivity) inside the molten chloride and collect the maximum rates of hydrocarbon products at atmospheric pressure. The rates of H_2 and CH_4 production, collected from the cathodic tube, changed significantly after the first 30 and 60 min of electrolysis due to the process of carbonate ions formation as can be seen by the comparison of **Fig. 4(a)** and **(b)**. Where the higher production rates of CH_4 (0.67 µmol/h cm^2) and H_2 (32.00 µmol/h cm^2) with higher faraday efficiency (59.30%) were found after the first 30 min of electrolysis (**Fig. 4(a)**). While the lower production rates of CH_4 (0.39 µmol/h cm^2) and H_2 (19.10 µmol/h cm^2) with faraday efficiency (30.50%) were obtained after 60 min of electrolysis (**Fig. 4(b)**) in molten chloride (LiCl-KCl; 41: 59 mol%).

The lower faraday efficiency (30.50%) was attributed due to the higher CO_3^{2-}ion formation leading to the subsequent conversion to C or CO with more energy consumption. The formation of a carbonate ion can be justified due to the reaction of CO_2 with OH^- generated in the molten chloride after the persistent reduction of H_2O as stated previously in **Eq. (10)** [46]. It is interesting to note that there is a clear increasing trend of CH_4 production in both **Fig. 4(a)** and **(b)** at a lower current density of 20 mA/cm^2, which starts dropping off beyond this limit. The increase in current density affects the products content. With the current density increase, the CH_4 production reached to an optimal value. After that further rise in current density results in

adverse effects on CH_4 production, greatly exceeding the minimum energy requirement of H_2 production that keeps CH_4 production at a lower level [24, 35]. Deng *et al.* [31] stated that LiCl-KCl electrolyte containing $Li_2CO_3/CaCO_3$ showed highest current efficiency of 80–85% at the current density of 25 mA/cm^2, which dropped off by increasing current density for the conversion of CO_2 to carbon.

Comparing results for the two occasions as two gas samples were taken after 30 and 60 min, it can be noted that the production rates of both gases (CH_4 and H_2) were higher in the first sample after first 30 min of electrolysis as the electro-reduction of the carbonate ions (to carbon for instance) had not commenced yet. Thus, the reduction of H_2O to H_2 was not significantly affected. The reaction of CO_2 with OH^- can be confirmed in the molten chloride for the second sample as the concentration of CO_2 reduced from 34.80 to 4.80% (**Table 1**).The hydrocarbon production confirmed through GC analysis (with FID and TCD detectors) is shown in **Fig. 5** where the FID signals are showing the production of methane with the peak at 2.11 retention time while TCD signals are clearly representing the peaks of H_2, O_2 and CO_2. No CO can be detected in the molten chloride in both cases.

Thus, the best product concentrations are obtained in case of LiCl-KCl (41: 59 mol%) electrolyte from GFIE mode at the first 30 min of electrolysis rather than prolonged electrolysis (60 min). This is because of the formation of carbonate ions in case of prolonged electrolysis, which are reduced to the C or CO gases with the consumption of more energy (**Table 1**). Ijije *et al.* [47] reported the CO_2 conversion into carbon films or CO in LiCl-KCl-$CaCl_2$-$CaCO_3$ molten salt at 520 ^oC. Similarly, the absorption and conversion of CO_2 was also employed in molten chloride electrolytes ($CaCl_2$-CaO and LiCl-Li_2O) at 900 and 650 ^oC respectively [48]. Jianbang *et al.* [30] has converted CO_2 by electrolysis in LiCl molten salt at 650 ^oC.

Molten hydroxide electrolyte

The molten hydroxide salt is preferred in the case of hydrogen production leading to hydrocarbons formation. Hydrocarbon molecules can be formed basically through a H_2 reaction with either C or CO as the same mechanism for molten chlorides [49]. In most experiments using molten hydroxides, the conversion of CO_2 was very high but the hydrocarbon yields were still low. This can be attributed generally to the reaction of CO_2 with hydroxide ions [50].

$$2OH^- + CO_2 \rightarrow CO_3^{2-} + H_2O \quad (14)$$

Therefore, CO_2 must be diluted to lower concentrations by mixing with argon gas before introduction to the electrolyte, as this action can help to reduce the reactivity of CO_2 with the salt, driving reaction (**Eq. (14)**) to the left side. The formation of carbonate ions need to be reduced to provide enough time for the prospect of electro-reduction during electrolysis. However, CH_4 gas can be formed by another way in case of molten hydroxide electrolysis (**Eq. (15)**) [51].

$$CO_2 + 4H_2 \rightarrow CH_4 + 2H_2O \quad (15)$$

Thus, the abundance of hydrogen gas from rapid H_2O reduction in molten hydroxides can contribute towards driving reaction (**Eq. (15)**) to CH_4 formation. The hydrocarbon production in molten hydroxide (LiOH-NaOH: 27: 73 mol%) performed in two modes: GFOE and GFIE at the conditions of 2 V applied voltage and 275 ºC, is shown in **Fig. 6 (a)** and **(b**). The results indicate a distinct variation in the production rates due to the variation in gas feed modes. This outcome can be attributed to the weak reduction of CO_2 in the salt in GFOE mode. The hydrocarbon production rate was significantly improved when the feed gas insertion method was changed from GFOE to GFIE. It can be seen from the **Fig. 6 (a)** to **(b)** that the CH_4 rate

increased largely from 1.02 to 6.12 μmol/h cm^2 by moving from GFOE to GFIE mode as CO_2 was promoted to dissolve in the salt.

Therefore, the prospect of direct reduction of CO_2 to CO_2^{2-} and CO can occur in the LiOH-NaOH salt. At the same time, the H_2 rate decreased from 1142.80 μmol/h cm^2 to just 185.00 μmol/h cm^2, confirming the possible transformation of CO_2 or CO to hydrocarbons. Nevertheless, high faraday efficiency (87.70%) in the GFOE mode rather than (15.00%) in the GFIE mode was due to the higher H_2 production rate. On the other hand, low faraday efficiencies in GFIE mode were obviously because of their lower production values from the slow reduction of CO_2 to CO compared with rapid H_2 production. Moreover, the optimal current density range found for hydrocarbon production in case of LiOH-NaOH salt was 80–85 mA/cm^2.

Hydrocarbon production inside the molten hydroxide can be confirmed actually by the existence of CO fuel with the cathode gas product. CO can be formed from CO_2 reduction as in molten chloride experiments. But the scarcity of CO gas found in the cathodic products in both electrolytes can be interpreted due to (1) a lack of CO_2 direct reduction to CO but the formation of CH_4 occurs by the reaction of CO_2 with excess H_2 and (2) the produced amount of CO during electrolysis in all cases was too little as CO can rapidly react with excess H_2 to produce CH_4. The formation of gaseous product (CH_4) was confirmed from GC analysis with FID detector while H_2, O_2 and CO_2 were confirmed by TCD detectors for the GFIE mode (**Fig. 7)**. And obtained values are presented in **Table 2**. The presence of very small peak of CO in **Fig. 7 (b)** is providing the indication of higher methane production rates than molten chloride case.

As the GFIE mode provided higher production values of methane in case of molten hydroxide so the experiment was repeated using KOH-NaOH (50:50 mol%) due to its low working temperature, under the conditions of 2V applied cell voltage and 225 ºC with GFIE mode only. Although the temperature used here was slightly lower than 275 ºC as used for LiOH-NaOH (27: 73 mol%) molten salt but the production rates of H_2 (164.70 µmol/h cm^2) and CH_4 (6.12 µmol/h cm^2) with faradaic efficiencies (17.90%) were almost same (**Fig. 6 (c)**). Moreover, the composition and concentration (vol%) of other cathodic product gases were also same (**Table 2**). But one limiting factor was the lower resulting current in the case of KOH-NaOH (50:50 mol%) molten salt than LiOH-NaOH (27: 73 mol%) (**Fig. 8)**. Moreover, the potentials for carbon deposition or carbon monoxide evolution are more positive than the deposition potentials of Li metal for the case of LiOH.

In contrast, in the case of KOH, the potential for the formation of C or CO is more negative than the deposition potential of potassium. The comparison suggests that carbon/CO evolution leading to the formation of methane is the more preferential product in the presence of LiOH as also observed in the previous study [44]. Therefore, the KOH-NaOH (50:50 mol%) electrolyte use was not preferred for hydrocarbon production. Consequently, the fuel production (H_2, CH_4) was achieved in all cases of molten hydroxide electrolytes with different product composition and concentration (vol%) as can be seen from **Table 2** but the best results were provided by the LiOH-NaOH (27: 73 mol%) molten salt with GFIE mode than the other cases.

Molten carbonate electrolyte

The third kind of electrolyte used for hydrocarbon production is a ternary molten carbonate mixture (Li_2CO_3-Na_2CO_3-K_2CO_3; 43.5: 31.5: 25.0 mol%) that is used in this research due to its relatively low melting point of 394 ºC. The formation of hydrocarbons can occur directly or indirectly in a molten carbonate through the reaction of C with H_2 or CO with H_2 respectively

which are produced primarily from the independent reductions of CO_2 and H_2O [28, 52]. Subsequently, experiments conducted on this salt at a range of 400–450 ºC, can be perfect conditions for efficient hydrocarbon formation. In the case of electrolysis applied at conditions of 1.5 V cell voltage and 425 ºC, the maximum CH_4 production rate was achieved. It can be seen from **Fig. 9** that a significant amount of CH_4 (1.10 µmol/h cm^2), H_2 (4.40 µmol/h cm^2) and CO (11.70 µmol/h cm^2) were obtained at the lower current density range of 4–6 mA/cm^2.

The relevant faraday efficiency obtained was 56.20% for the production of CH_4, CO and H_2, which were confirmed through GC analysis using FID and TCD detectors (see **Fig. 10**) with production concentration values mention in **Table 3**. These production results are in agreement with previous studies [24, 25]. Wu et al. [10] provided support to the conversion of CO_2 and H_2O to methane in case of molten carbonate electrolysis. It is worth mentioning that H_2 and CO were the predominant gases during the experiment. Moreover, the existence of CO as clearly noted from **Fig. 9** and confirmed through GC analysis with TCD detector (see **Fig. 10 (b))** in a relatively significant amount (in comparison to CH_4), can be imputed to the individual reduction of CO_2 to CO. Previous studies stated that CO itself cannot be expected in molten carbonates at temperatures below 775 ºC in cases where H_2O is absent [40].

However, some other authors have claimed that the formation of CO molecules can occur on the cathode by CO_2 reduction at low temperatures (≤ 650 °C) [53]. If the reduction of CO_2 to CO is preferred, then H_2 gas will also be formed according to the water gas shift reaction (WGSR) which occurs due to higher temperature (< 600 ºC). In contrast, CO can be generated by the reverse water gas shift reaction (RWGS) [50]. However, WGSR is more feasible at temperatures below 817 ºC particularly in the event of high partial pressures of H_2O (up to 16.1 mmHg) which is not the condition of present study case, so CO formation is preferred case than the H_2

production leading to the hydrocarbon production. The only GFIE mode is presented here due to the same results obtained in both cases (GFOE and GFIE mode) because of the excessive CO_3^{2-} ions already present in Li_2CO_3-Na_2CO_3-K_2CO_3 (43.5: 31.5: 25.0 mol%).

The existence of CO_2 gas in the cathodic gas products in all the molten electrolyte cases can be due to the reasons as (1) some of the absorbed CO_2 from the molten carbonates can come out with the cathodic product gas (2) CO_2 can be produced accompanying the various hydrocarbon species (3) The difference between the inlet and outlet amounts of CO_2 cannot be ultimately accounted as the transferred CO_2 to CO and hydrocarbon products. Some other amounts of CO_2 can be absorbed chemically in the molten salts (4) The 100 % CO_2 gas conversion cannot be done. However, in large scale applications, the cathodic product gas with accompanied amounts of CO_2 can be recycled repeatedly with feed gas to increase the ultimate CO_2 conversion rate. Ji *et al.* [35] was able to convert CO_2 and H_2O into CO, H_2 and CH_4 products at 600 ºC with the current efficiency of 51% in Li-Na-KCO_3-0.3LiOH electrolyte.

Effect of temperature and voltage

The optimum temperature used for the selected molten hydroxides was chosen on the basis of the maximum CH_4 production obtained as can be seen from **Fig. 11**. The optimum temperatures obtained were 375, 275, 225 and 425 ºC for KCl-LiCl (58.5: 41.5 mol%), KOH-NaOH (50: 50 mol%), LiOH-NaOH (27: 73 mol%) and Li_2CO_3-Na_2CO_3-K_2CO_3 (43.5: 31.5 :25 mol%) electrolytes respectively. The yields of hydrocarbon products (vol%) increased with the rise in temperature up to an optimum temperature value while after that further rise in temperature showed inverse effects in case of molten hydroxide and chloride salts. This was because the CO_2 could not be transferred significantly to CO or hydrocarbon species because of the prospects chemisorption of CO_2 in molten electrolytes at higher temperature. Ji *et al.* [35]

provided the support to the obtained results by reporting that the reduction of co-electrolysis of CO_2 and H_2O decreases by increasing the temperature.

While in the case of Li_2CO_3-Na_2CO_3-K_2CO_3, the highest CH_4 production increased up to 425 ^oC while after this temperature CH_4 production starts decreasing which might be due to the increase in production values of other longer chain hydrocarbons (C_2-C_4) rather than CH_4 only. This can be due to the increase in CO_2 gas solubility inside molten chloride at high temperature (475 ^oC) [54]. The cell voltage is a key variable that can affect energy consumption or current efficiency but it can also improve the product properties at the same time [49, 54]. In case of molten chlorides and hydroxides, the average current density increased drastically (20 to 70 mA/cm^2) and (70 to 120 mA/cm^2) by increasing cell voltage from 2V to 3V as shown in **Fig. 12(a)** and **(b).** Likewise, CH_4 concentration (vol%) increased but with slower production rates.

However, the alkali metal electrodeposition starts occurring at a high cell voltage, consequently affecting the current efficiencies of the products. So, at higher voltage, there is more waste of energy due to the solid metal accumulation than the desired products [55]. Therefore, the optimum voltage selected for molten chlorides and hydroxides was 2V rather than 3V. To show the effect of increasing cell voltage in molten carbonates, **Fig. 12(c)** illustrates the high difference between the average current (4 to 25 mA/cm^2) resulting from electrolysis applied at 1.5 and 2 V. The hydrocarbon formation was confirmed only at 1.5 V while carbon deposition occurred due to the rise of voltage up to 2 V as also confirmed by previous studies [54, 56]. Performing both runs at 425 ^oC, hydrocarbon formation at 2 V was rare and not noticeable. Consequently, the optimum voltage selected for molten chloride and molten hydroxide was 2 V while 1.5 V for molten carbonates.

Formation of higher hydrocarbons

The GC analysis performed using FID detector (**Fig. 10(a)**) showed that along with methane production, various higher hydrocarbons were also detected in the case of molten carbonate electrolyte. Which is further confirmed by GC-MS analysis (**Fig. 14)**. The formation of methane gas product can be justified due to the reaction of carbon or CO with H_2 as follows:

$$C + 2H_2 \rightarrow CH_4 \qquad \Delta G_{425C} = -49.5\ \text{kJmol}^{-1} \qquad (16)$$

$$CO + 3H_2 \rightarrow CH_4 + H_2O\ (g) \qquad \Delta G_{425C} = -49.5\ \text{kJmol}^{-1} \qquad (17)$$

$$2CO + 2H_2 \rightarrow CH_4 + CO_2\ (g) \qquad \Delta G_{425C} = -68.4\ \text{kJmol}^{-1} \qquad (18)$$

The Gibbs Energy values were determined at 425 ºC (HSC Chemistry software, version 6.12; Outokumpu Research) as this was the temperature of the experiment. It can be seen from the first mechanism that the production of general hydrocarbons occurs basically from reaction in **Eq. (16)** with the fresh deposit of carbon and adsorbed atomic hydrogen (H), produced in turn from the individual reduction of CO_2 and H_2O respectively. On the other hand, the C_2, C_3 and C_4 hydrocarbons, detected by GC analysis (with FID detector) are shown in **Fig. 13** along with their production rate values (0.80, 0.50, 0.50 μmol/h.cm^2) and faradays efficiency (total = 55.20%). It is important to note that the accumulative faraday efficiency for all products (C_1, C_2, C_3, C_4, CO and H_2) obtained in case of molten carbonates electrolysis reached to the 95% **(Table 3)**.

The dominant peaks were of alkene products rather than alkanes in the GC analysis when detected with FID detector, such as for ethene, propene, butene and pentene at 2.73, 3.06, 7.71 and 18.11 of retention times respectively. However, GC-MS analysis are also showing the detection for some alkane products. The formation of alkene or alkanes can be justified due to

the (1) reaction of C or CO with hydrogen or (2) partial oxidation of methane in molten carbonate. Furthermore, in the first mechanism the CO produced in excess can react with H_2 gas to produce higher hydrocarbons (C_2, C_3, and C_4) through two different routes. The first set of reactions (**Eqs. (19-20)**) results in H_2O generation [57, 58] whereas the second set (**Eqs. (21-22)**) produces CO_2 instead [59]. The CO_2 by-product method is more feasible than the method with H_2O formation as shown in **Table 4.**

$$nCO + (2n + 1)H_2 \rightarrow C_nH_{2n+2} + nH_2O \quad (19)$$

$$nCO + 2nH_2 \rightarrow C_nH_{2n} + nH_2O \quad (20)$$

$$2nCO + (n + 1)H_2 \rightarrow C_nH_{2n+2} + nCO_2 \quad (21)$$

$$2nCO + nH_2 \rightarrow C_nH_{2n} + nCO_2 \quad (22)$$

Alkane and alkene products in general are generated primarily through the CO_2 route particularly in media where CO_2 is highly absorbed (molten carbonates). The absorption of some amounts of generated CO_2 can be sustained in the molten salt, driving the reactions (**Eqs. (21-22)**) to the right side and increasing hydrocarbon formation. Moreover, due to the primary production of higher CO rates and in contrast lower H_2 rates, alkene hydrocarbons were found in a higher proportion than the corresponding alkanes in the final cathodic product. The ΔG data values (**Table 4)** confirm that the formation of higher hydrocarbon molecules (C_2-C_4) was possible through the production of CO_2 for alkanes rather than alkenes by the process of Fischer Tropsch reaction.

Therefore, as far as adequate amounts of CO and H_2 gases are produced from electrolysis, there is sufficient availability for combining on the cathode surface producing alkanes. While the justification for the formation of alkenes such as C_2H_4, C_3H_6, C_4H_8, rather than alkanes can be

provided by the partial oxidation of CH_4 gas. These conditions hold true particularly at a lower CO_2 absorption level due to the feasible partial oxidation of CH_4 to C_2H_4 rather than C_2H_6.

$$2CH_4 + O_2 \rightarrow C_2H_4 + 2H_2O \qquad \Delta G_{425C} = -297\ kJmol^{-1} \qquad (23)$$

$$2CH_4 + 1/2\ O_2 \rightarrow C_2H_6 + H_2O \qquad \Delta G_{425C} = -138\ kJmol^{-1} \qquad (24)$$

The oxidation of CH_4 can be performed in two ways. Firstly, CH_4 gas can react directly with O_2 formed at the anode during the co-electrolysis of CO_2 and H_2O (**Eqs. (23-24)**) or also can react with O_2 absorbed inside the molten salt for a short time prior to passing through the anode ceramic tube or being eluted with the cathodic gas product by the draft of feed gas. Secondly, the absorbed O_2 can be transferred to a more reactive oxide anion like peroxide (diatomic O_2^{2-} or monoatomic O^-), playing a significant role in the methane oxidation mechanism particularly in the case of low CO_2 concentration levels. It can also be seen from ***Table 4*** that the formation of higher molecular weight hydrocarbons (>C_2) will be more feasible (resulting in a more negative ΔG) by this mechanism with the priority on alkenes rather than alkanes.

The formation of C_2H_6, C_3H_8 and C_4H_{10} was relatively small compared with the corresponding alkenes as also seen by GC-MS analysis (**Fig. 14)** as the peaks 57, 43 and 29 stands for the mass of fragments lost from C_4H_{10} ($CH_3CH_2CH_2CH_3$), C_3H_8 ($CH_3CH_2CH_3$) and C_2H_6 (CH_3CH_3) respectively. The last peaks (43 and 29) are produced from the further fragmentation of C_3H_8 and C_4H_{10}. Peaks 55 and 41 stands for the mass of fragments lost from 1-C_4H_8 (for instance) and C_3H_6 respectively. Peak 15 is showing the mass fragment (methyl) lost from C_4H_{10}, C_3H_8 and C_2H_6. Branco *et al.* [60, 61] also stated the higher hydrocarbon production (C_2-C_4) through partial oxidation of methane in molten salt electrolytes.

Energy consumption and heating values

The energy required for the conversion of CO_2 to carbon/hydrocarbons will be that needed to carry out the electrolysis and heating up of the molten salt [45]. If the heating values or energy supplied from the produced fuels are able to compensate some or all the energy consumed while performing electrolysis, the process feasibility increases[62]. This is because the yield of heat generated from the produced hydrocarbon fuel can compensate or substitute some of the normal electricity employed in large scale industrial applications. In the case of molten chloride (KCl-LiCl; 41–59 mol%) electrolyte, the heating value obtained is 162 J from the produced fuel (H_2 and CH_4) with the energy consumption of 278 J. While the heating values obtained are 136 and 170 J from the produced fuels (H_2 and CH_4) by using KOH-NaOH (50: 50 mol%) and LiOH-NaOH (27:73 mol%) respectively. And with the energy consumption of 1200 and 1000 J in KOH-NaOH (50: 50 mol%) and LiOH-NaOH (27:73 mol%) electrolysis respectively (see **Table 2**).

The greater the production of higher hydrocarbons (C_1-C_4), the greater the faraday efficiency and subsequent energy profit attained due to their ability to produce more heating energy **(Table 3).** It is very interesting to note that the energy obtained from the summation of heating values of cathodic products in Li_2CO_3-Na_2CO_3-K_2CO_3 (43.5 : 31.5 : 25 mol%) case was 94.6 J while the total consumed energy was 114.2 J with about 100% of faraday efficiency **(Table 3)**. The higher total efficiency results in significantly lower energy consumption of 114 J for the total fuel produced or just 0.157 kWh per mole of fuel. This value is apparently less than the energy consumed for an optimum deposit carbon operation of 0.456 kWh per mole of carbon [56]. As in all the cases, the produced hydrocarbon fuels are able to provide sufficient heating values so the CO_2-H_2O co-electrolysis processes are considered successful. Tang *et al.* [54] has

optimized energy consumption for producing 1 kg of carbon from CO_2 as low as 35.59 kW h with a current efficiency of 87.86% under a constant cell voltage of 3.5 V in molten carbonates.

Conclusions

This study presents a new method of CO_2-H_2O conversion into hydrocarbon fuel via molten salts electrolysis at relatively low temperature that is a dire need of hydrocarbon production. The synthesis method generated methane and hydrogen gases by a direct simultaneous splitting of CO_2 and H_2O in LiCl-KCl (58.5: 41.5 mol%), LiOH-NaOH (27: 73 mol%), KOH-NaOH (50: 50 mol%) and Li_2CO_3-Na_2CO_3-K_2CO_3 (43.5 : 31.5 : 25 mol%) electrolyte mixtures. The optimization of each electrolyte was done in the gas feed introduction method (GFOE and GFIE) for obtaining more fuel production. In the case of KCl-LiCl (41: 59 mol%), CH_4 (0.67 μmol/h.cm^2) and H_2 (32 μmol/h.cm^2) were produced with GFIE mode at atmospheric pressure. While in molten hydroxide (LiOH-NaOH; 27: 73 mol %), the H_2 was the predominant gas due to H_2O electrolysis which contributed majorly to the production of CH_4 by reacting with CO_2. The hydrocarbon production rate increased (CH_4: 1.02 to 6.12 μmol h/cm^2) by changing the feed gas insertion mode from GFOE to GFIE by using a ceramic tube. In case of molten carbonate, the production rate of CO (11.70 μmol/h.cm^2) was significantly higher than H_2 (4.40 μmol/h.cm^2) in cathodic gas product. Along with H_2 and CO, other hydrocarbon species such as CH_4 and olefins were also produced in molten carbonate case with 99 % of faraday efficiency while other being 59.30% and 87.70% in molten chloride and molten hydroxides respectively. Moreover, the suitable conditions at which the fuel production was achievable are 375 ^oC, 275 ^oC and 475 ^oC for molten chlorides, molten hydroxides and molten carbonates under the cell voltage of 2V, 2V and 1.5 V respectively. The proposed technique holds promise as a method for converting electrical energy produced from renewable power sources into conventional fuel, this should be used in future with increased production concentrations.

Supporting information

Phase diagram in mole percentages for binary mixtures of (a) chloride (LiCl-KCl) (b) hydroxide (LiOH-NaOH) and (c) hydroxide (KOH-NaOH) salts (**Fig. S1**) and phase diagram of Li_2CO_3-Na_2CO_3 -K_2CO_3 ternary molten salt (**Fig. S2**).

Acknowledgement

The authors are grateful for the financial supports from the EPSRC (EP/J000582/1 and EP/F026412/1) and Ningbo Municipal People's Governments (3315 Plan and 2014A35001-1).

References

1. Lei, L.; Liu, T.; Fang, S.; Lemmon, J. P.; Chen, F., The co-electrolysis of CO 2–H 2 O to methane via a novel micro-tubular electrochemical reactor. *J. Mater. Chem. A* 2017, *5* (6), 2904-2910, DOI 10.1039/C6TA10252B.
2. Ren, J.; Yu, A.; Peng, P.; Lefler, M.; Li, F.-F.; Licht, S., Recent Advances in Solar Thermal Electrochemical Process (STEP) for Carbon Neutral Products and High Value Nanocarbons. *Acc. Chem. Res.* 2019, *52* (11), 3177-3187, DOI 10.1021/acs.accounts.9b00405.
3. Christensen, E.; Petrushina, I.; Nikiforov, A. V.; Berg, R. W.; Bjerrum, N. J., CsH2PO4 as Electrolyte for the Formation of CH4 by Electrochemical Eeduction of CO2. *J. Electrochem. Soc.* 2020, *167* (4), 044511, DOI 10.1149/1945-7111/ab75fa.
4. Skafte, T. L.; Blennow, P.; Hjelm, J.; Graves, C., Carbon deposition and sulfur poisoning during CO2 electrolysis in nickel-based solid oxide cell electrodes. *J. Power Sources* 2018, *373*, 54-60, DOI 10.1016/j.jpowsour.2017.10.097.
5. Sher, F.; Iqbal, S. Z.; Liu, H.; Imran, M.; Snape, C. E., Thermal and kinetic analysis of diverse biomass fuels under different reaction environment: A way forward to renewable energy sources. *Energy Convers. Manage.* 2020, *203*, 112266, DOI 10.1016/j.enconman.2019.112266.
6. Abu Hassan, M. H.; Sher, F.; Zarren, G.; Suleiman, N.; Tahir, A. A.; Snape, C. E., Kinetic and thermodynamic evaluation of effective combined promoters for CO2 hydrate formation. *J. Nat. Gas Sci. Eng.* 2020, *78*, 103313, DOI 10.1016/j.jngse.2020.103313.
7. Kumaravel, V.; Bartlett, J.; Pillai, S. C., Photoelectrochemical conversion of carbon dioxide (CO2) into fuels and value-added products. *ACS Energy Lett.* 2020, DOI 10.1021/acsenergylett.9b02585.
8. Anwar, M.; Fayyaz, A.; Sohail, N.; Khokhar, M.; Baqar, M.; Yasar, A.; Rasool, K.; Nazir, A.; Raja, M.; Rehan, M., CO2 utilization: Turning greenhouse gas into fuels and valuable products. *J. Environ. Manage.* 2020, *260*, 110059, DOI 10.1016/j.jenvman.2019.110059.
9. Sastre, F.; Muñoz-Batista, M. J.; Kubacka, A.; Fernández-García, M.; Smith, W. A.; Kapteijn, F.; Makkee, M.; Gascon, J., Efficient Electrochemical Production of Syngas from CO2 and H2O by using a Nanostructured Ag/g-C3N4 Catalyst. *ChemElectroChem* 2016, *3* (9), 1497-1502, DOI 10.1002/celc.201600392.
10. Wu, H.; Ji, D.; Li, L.; Yuan, D.; Zhu, Y.; Wang, B.; Zhang, Z.; Licht, S., A new technology for efficient, high yield carbon dioxide and water transformation to methane by electrolysis in molten salts. *Adv. Mater. Technol.* 2016, *1* (6), 1600092, DOI 10.1002/admt.201600092.
11. Li, Z.; Zhang, W.; Ji, D.; Liu, S.; Cheng, Y.; Han, J.; Wu, H., Electrochemical Conversion of CO2 into Valuable Carbon Nanotubes: The Insights into Metallic Electrodes Screening. *J. Electrochem. Soc.* 2020, *167* (4), 042501, DOI 10.1149/1945-7111/ab7176.
12. Long, C.; Li, X.; Guo, J.; Shi, Y.; Liu, S.; Tang, Z., Electrochemical reduction of CO2 over heterogeneous catalysts in aqueous solution: recent progress and perspectives. *Small Methods* 2019, *3* (3), 1800369, DOI 10.1002/smtd.201800369.
13. Moura de Salles Pupo, M.; Kortlever, R., Electrolyte effects on the electrochemical reduction of CO2. *ChemPhysChem* 2019, *20* (22), 2926-2935, DOI 10.1002/cphc.201900680.
14. Chen, Y.; Wang, M.; Lu, S.; Tu, J.; Jiao, S., Electrochemical graphitization conversion of CO2 through soluble NaVO3 homogeneous catalyst in carbonate molten salt. *Electrochim. Acta* 2020, *331*, 135461, DOI 10.1016/j.electacta.2019.135461.
15. Kusama, S.; Saito, T.; Hashiba, H.; Sakai, A.; Yotsuhashi, S., Crystalline copper (II) phthalocyanine catalysts for electrochemical reduction of carbon dioxide in aqueous media. *ACS Catal.* 2017, *7* (12), 8382-8385, DOI 10.1021/acscatal.7b02220.

16. Acar, C.; Dincer, I., Review and evaluation of hydrogen production options for better environment. *J. Cleaner Prod.* 2019, *218*, 835-849, DOI 10.1016/j.jclepro.2019.02.046.
17. Al-Shara, N. K.; Sher, F.; Iqbal, S. Z.; Curnick, O.; Chen, G. Z., Design and optimization of electrochemical cell potential for hydrogen gas production. *J. Energy Chem.* 2021, *52*, 421-427, DOI 10.1016/j.jechem.2020.04.026.
18. Luo, Y.; Shi, Y.; Chen, Y.; Li, W.; Jiang, L.; Cai, N., Pressurized Tubular Solid Oxide H2O/CO2 Co-electrolysis Cell for Direct Power-to-Methane. *AlChE J.* 2020, e16896, DOI 10.1002/aic.16896.
19. Kamali, A. R., Production of Advanced Materials in Molten Salts. In *Green Production of Carbon Nanomaterials in Molten Salts and Applications*, Springer: 2020; pp 5-18, DOI 10.1007/978-981-15-2373-1_2.
20. Dogu, D.; Gunduz, S.; Meyer, K. E.; Deka, D. J.; Ozkan, U. S., CO 2 and H 2 O Electrolysis Using Solid Oxide Electrolyzer Cell (SOEC) with La and Cl-doped Strontium Titanate Cathode. *Catal. Lett.* 2019, *149* (7), 1743-1752, DOI 10.1007/s10562-019-02786-8.
21. Wu, H.; Liu, Y.; Ji, D.; Li, Z.; Yi, G.; Yuan, D.; Wang, B.; Zhang, Z.; Wang, P., Renewable and high efficient syngas production from carbon dioxide and water through solar energy assisted electrolysis in eutectic molten salts. *J. Power Sources* 2017, *362*, 92-104, DOI 10.1016/j.jpowsour.2017.07.016.
22. Xu, H.; Chen, B.; Irvine, J.; Ni, M., Modeling of CH4-assisted SOEC for H2O/CO2 co-electrolysis. *Int. J. Hydrogen Energy* 2016, *41* (47), 21839-21849, DOI 10.1016/j.ijhydene.2016.10.026.
23. Tang, D.; Dou, Y.; Yin, H.; Mao, X.; Xiao, W.; Wang, D., The capacitive performances of carbon obtained from the electrolysis of CO2 in molten carbonates: Effects of electrolysis voltage and temperature. *J. Energy Chem.* 2019, DOI 10.1016/j.jechem.2019.11.006.
24. Ji, D.; Li, Z.; Li, W.; Yuan, D.; Wang, Y.; Yu, Y.; Wu, H., The optimization of electrolyte composition for CH4 and H2 generation via CO2/H2O co-electrolysis in eutectic molten salts. *Int. J. Hydrogen Energy* 2019, *44* (11), 5082-5089, DOI 10.1016/j.ijhydene.2018.09.089.
25. Liu, Y.; Ji, D.; Li, Z.; Yuan, D.; Jiang, M.; Yang, G.; Yu, Y.; Wang, Y.; Wu, H., Effect of CaCO3 addition on the electrochemical generation of syngas from CO2/H2O in molten salts. *Int. J. Hydrogen Energy* 2017, *42* (29), 18165-18173, DOI 10.1016/j.ijhydene.2017.04.160.
26. Xiao, W.; Wang, D.-H., Rare metals preparation by electro-reduction of solid compounds in high-temperature molten salts. *Rare Met.* 2016, *35* (8), 581-590, DOI 10.1007/s12598-016-0778-4.
27. Ijije, H. V.; Sun, C.; Chen, G. Z., Indirect electrochemical reduction of carbon dioxide to carbon nanopowders in molten alkali carbonates: Process variables and product properties. *Carbon* 2014, *73*, 163-174, DOI 10.1016/j.carbon.2014.02.052.
28. Liu, Y.; Yuan, D.; Ji, D.; Li, Z.; Zhang, Z.; Wang, B.; Wu, H., Syngas production: diverse H 2/CO range by regulating carbonates electrolyte composition from CO 2/H 2 O via co-electrolysis in eutectic molten salts. *RSC Adv.* 2017, *7* (83), 52414-52422, DOI 10.1039/C7RA07320H.
29. Weng, W.; Tang, L.; Xiao, W., Capture and electro-splitting of CO2 in molten salts. *J. Energy Chem.* 2019, *28*, 128-143, DOI 10.1016/j.jechem.2018.06.012.
30. Ge, J.; Hu, L.; Wang, W.; Jiao, H.; Jiao, S., Electrochemical Conversion of CO2 into Negative Electrode Materials for Li-Ion Batteries. *ChemElectroChem* 2015, *2* (2), 224-230, DOI 10.1002/celc.201402297.
31. Deng, B.; Chen, Z.; Gao, M.; Song, Y.; Zheng, K.; Tang, J.; Xiao, W.; Mao, X.; Wang, D., Molten salt CO2 capture and electro-transformation (MSCC-ET) into capacitive

carbon at medium temperature: effect of the electrolyte composition. *Faraday Discuss.* 2016, *190*, 241-258, DOI 10.1039/C5FD00234F.
32. Ren, J.; Johnson, M.; Singhal, R.; Licht, S., Transformation of the greenhouse gas CO2 by molten electrolysis into a wide controlled selection of carbon nanotubes. *J. CO2 Util.* 2017, *18*, 335-344, DOI 10.1016/j.jcou.2017.02.005.
33. Douglas, A.; Carter, R.; Muralidharan, N.; Oakes, L.; Pint, C. L., Iron catalyzed growth of crystalline multi-walled carbon nanotubes from ambient carbon dioxide mediated by molten carbonates. *Carbon* 2017, *116*, 572-578, DOI 10.1016/j.carbon.2017.02.032.
34. Arcaro, S.; Berutti, F.; Alves, A.; Bergmann, C., MWCNTs produced by electrolysis of molten carbonate: Characteristics of the cathodic products grown on galvanized steel and nickel chrome electrodes. *Appl. Surf. Sci.* 2019, *466*, 367-374, DOI 10.1016/j.apsusc.2018.10.055.
35. Ji, D.; Liu, Y.; Li, Z.; Yuan, D.; Yang, G.; Jiang, M.; Wang, Y.; Yu, Y.; Wu, H., A comparative study of electrodes in the direct synthesis of CH4 from CO2 and H2O in molten salts. *Int. J. Hydrogen Energy* 2017, *42* (29), 18156-18164, DOI 10.1016/j.ijhydene.2017.04.152.
36. Li, L.; Shi, Z.; Gao, B.; Hu, X.; Wang, Z., Electrochemical conversion of CO2 to carbon and oxygen in LiCl–Li2O melts. *Electrochim. Acta* 2016, *190*, 655-658, DOI 10.1016/j.electacta.2015.12.202.
37. Kaplan, V.; Wachtel, E.; Gartsman, K.; Feldman, Y.; Lubomirsky, I., Conversion of CO2 to CO by electrolysis of molten lithium carbonate. *J. Electrochem. Soc.* 2010, *157* (4), B552-B556, DOI 10.1149/1.3308596.
38. Ijije, H. V. Electrochemical conversion of carbon dioxide to carbon in molten carbonate salts. University of Nottingham, Cenrtal Store, 2015.
39. Hu, L.; Song, Y.; Ge, J.; Zhu, J.; Han, Z.; Jiao, S., Electrochemical deposition of carbon nanotubes from CO 2 in CaCl 2–NaCl-based melts. *J. Mater. Chem. A* 2017, *5* (13), 6219-6225, DOI 10.1039/C7TA00258K.
40. Lorenz, P. K.; Janz, G. J., Electrolysis of molten carbonates: anodic and cathodic gas-evolving reactions. *Electrochim. Acta* 1970, *15* (6), 1025-1035, DOI 10.1016/0013-4686(70)80042-1.
41. Halmann, M.; Zuckerman, K., Electroreduction of carbon dioxide to carbon monoxide in molten LiCl + KCl, LiF + KF + NaF, Li2CO3 + Na2CO3 + K2CO3 and AlCl3 + NaCl. *J. Electroanal. Chem. Interfacial Electrochem.* 1987, *235* (1), 369-380, DOI 10.1016/0022-0728(87)85221-X.
42. Al-Shara, N. K.; Sher, F.; Yaqoob, A.; Chen, G. Z., Electrochemical investigation of novel reference electrode Ni/Ni(OH)$_2$ in comparison with silver and platinum inert quasi-reference electrodes for electrolysis in eutectic molten hydroxide. *Int. J. Hydrogen Energy* 2019, *44* (50), 27224-27236, DOI 10.1016/j.ijhydene.2019.08.248.
43. Song, Q.; Xu, Q.; Wang, Y.; Shang, X.; Li, Z., Electrochemical deposition of carbon films on titanium in molten LiCl–KCl–K2CO3. *Thin Solid Films* 2012, *520* (23), 6856-6863, DOI 10.1016/j.tsf.2012.07.056.
44. Deng, B.; Tang, J.; Gao, M.; Mao, X.; Zhu, H.; Xiao, W.; Wang, D., Electrolytic synthesis of carbon from the captured CO2 in molten LiCl–KCl–CaCO3: Critical roles of electrode potential and temperature for hollow structure and lithium storage performance. *Electrochim. Acta* 2018, *259*, 975-985 DOI 10.1016/j.electacta.2017.11.025.
45. Ijije, H. V.; Lawrence, R. C.; Chen, G. Z., Carbon electrodeposition in molten salts: electrode reactions and applications. *RSC Adv.* 2014, *4* (67), 35808-35817, DOI 10.1039/C4RA04629C.

46. Kamali, A. R.; Fray, D. J., Large-scale preparation of graphene by high temperature insertion of hydrogen into graphite. *Nanoscale* 2015, *7* (26), 11310-11320, DOI 10.1039/C5NR01132A
47. Ijije, H. V.; Lawrence, R. C.; Siambun, N. J.; Jeong, S. M.; Jewell, D. A.; Hu, D.; Chen, G. Z., Electro-deposition and re-oxidation of carbon in carbonate-containing molten salts. *Faraday Discuss.* 2014, *172*, 105-116, DOI 10.1039/C4FD00046C.
48. Otake, K.; Kinoshita, H.; Kikuchi, T.; Suzuki, R. O., CO2 gas decomposition to carbon by electro-reduction in molten salts. *Electrochim. Acta* 2013, *100*, 293-299, DOI 10.1016/j.electacta.2013.02.076.
49. Al-Shara, N. K.; Sher, F.; Iqbal, S. Z.; Sajid, Z.; Chen, G. Z., Electrochemical study of different membrane materials for the fabrication of stable, reproducible and reusable reference electrode. *J. Energy Chem.* 2020, *49*, 33-41, DOI 10.1016/j.jechem.2020.01.008.
50. Graves, C.; Ebbesen, S. D.; Mogensen, M.; Lackner, K. S., Sustainable hydrocarbon fuels by recycling CO2 and H2O with renewable or nuclear energy. *Renewable Sustainable Energy Rev.* 2011, *15* (1), 1-23, DOI 10.1016/j.rser.2010.07.014.
51. Pardo, P.; Deydier, A.; Anxionnaz-Minvielle, Z.; Rougé, S.; Cabassud, M.; Cognet, P., A review on high temperature thermochemical heat energy storage. *Renewable Sustainable Energy Rev.* 2014, *32*, 591-610, DOI 10.1016/j.rser.2013.12.014.
52. Groult, H.; Le Van, K.; Lantelme, F., Electrodeposition of carbon-metal powders in alkali carbonate melts. *J. Electrochem. Soc.* 2014, *161* (7), D3130-3138, DOI 10.1149/2.019407jes.
53. Chery, D.; Albin, V.; Meléndez-Ceballos, A.; Lair, V.; Cassir, M., Mechanistic approach of the electrochemical reduction of CO2 into CO at a gold electrode in molten carbonates by cyclic voltammetry. *Int. J. Hydrogen Energy* 2016, *41* (41), 18706-18712 DOI 10.1016/j.ijhydene.2016.06.094.
54. Tang, D.; Yin, H.; Mao, X.; Xiao, W.; Wang, D., Effects of applied voltage and temperature on the electrochemical production of carbon powders from CO2 in molten salt with an inert anode. *Electrochim. Acta* 2013, *114*, 567-573, DOI 10.1016/j.electacta.2013.10.109.
55. Novoselova, I. A.; Kuleshov, S. V.; Volkov, S. V.; Bykov, V. N., Electrochemical synthesis, morphological and structural characteristics of carbon nanomaterials produced in molten salts. *Electrochim. Acta* 2016, *211*, 343-355, DOI 10.1016/j.electacta.2016.05.160.
56. Yin, H.; Mao, X.; Tang, D.; Xiao, W.; Xing, L.; Zhu, H.; Wang, D.; Sadoway, D. R., Capture and electrochemical conversion of CO 2 to value-added carbon and oxygen by molten salt electrolysis. *Energy Environ. Sci.* 2013, *6* (5), 1538-1545, DOI 10.1039/C3EE24132G.
57. Akhmedov, V.; Ismailzadeh, A., The role of CO 2 and H 2 O in the formation of gas-oil hydrocarbons: current performance and outlook. *J. Math* 2019, *6* (10).
58. Torrente-Murciano, L.; Mattia, D.; Jones, M. D.; Plucinski, P. K., Formation of hydrocarbons via CO2 hydrogenation – A thermodynamic study. *J. CO2 Util.* 2014, *6*, 34-39, DOI 10.1016/j.jcou.2014.03.002.
59. Jafarbegloo, M.; Tarlani, A.; Mesbah, A. W.; Sahebdelfar, S., Thermodynamic analysis of carbon dioxide reforming of methane and its practical relevance. *Int. J. Hydrogen Energy* 2015, *40* (6), 2445-2451, DOI 10.1016/j.ijhydene.2014.12.103.
60. Branco, J. B.; Lopes, G.; Ferreira, A. C.; Leal, J. P., Catalytic oxidation of methane on KCl-MClx (M= Li, Mg, Co, Cu, Zn) eutectic molten salts. *J. Mol. Liq.* 2012, *171*, 1-5, DOI 10.1016/j.molliq.2012.04.001.
61. Branco, J. B.; Lopes, G.; Ferreira, A. C., Catalytic oxidation of methane over KCl-LnCl3 eutectic molten salts. *Catal. Commun.* 2011, *12* (15), 1425-1427, DOI 10.1016/j.catcom.2011.05.023.

62. Al-Juboori, O.; Sher, F.; Hazafa, A.; Khan, M. K.; Chen, G. Z., The effect of variable operating parameters for hydrocarbon fuel formation from CO2 by molten salts electrolysis. *J. CO2 Util.* 2020, *40*, 101193, DOI 10.1016/j.jcou.2020.101193.

List of Figures

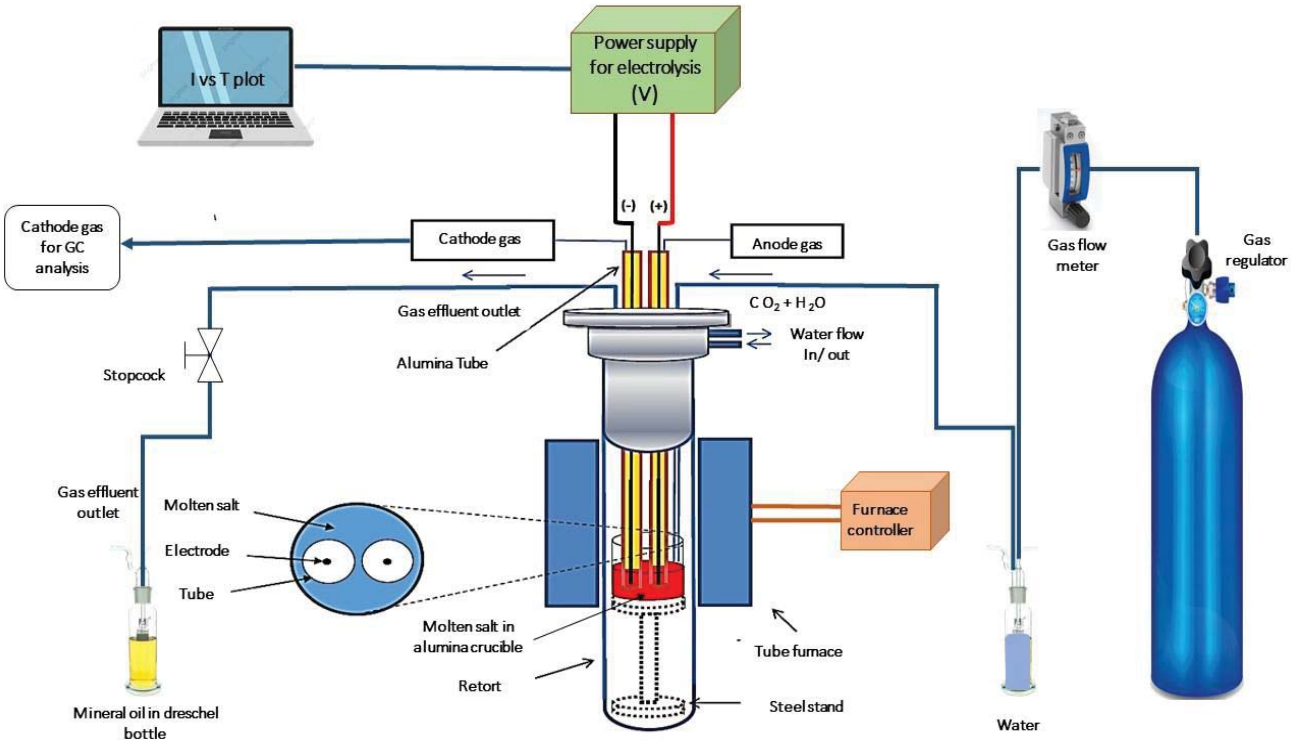

Fig. 1. A schematic representation of the experimental setup.

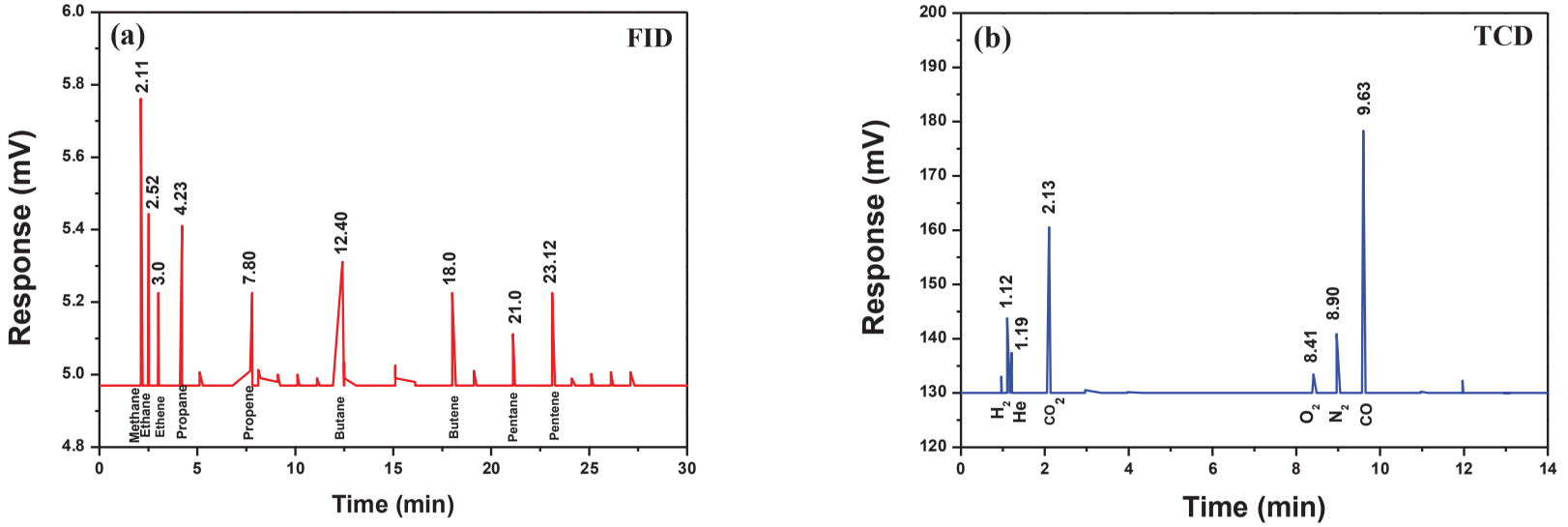

Fig. 2. The gas chromatography analysis of calibration gas standards as reference for the comparison with other electrolysis gaseous products by (a) FID detector (b) TCD detector.

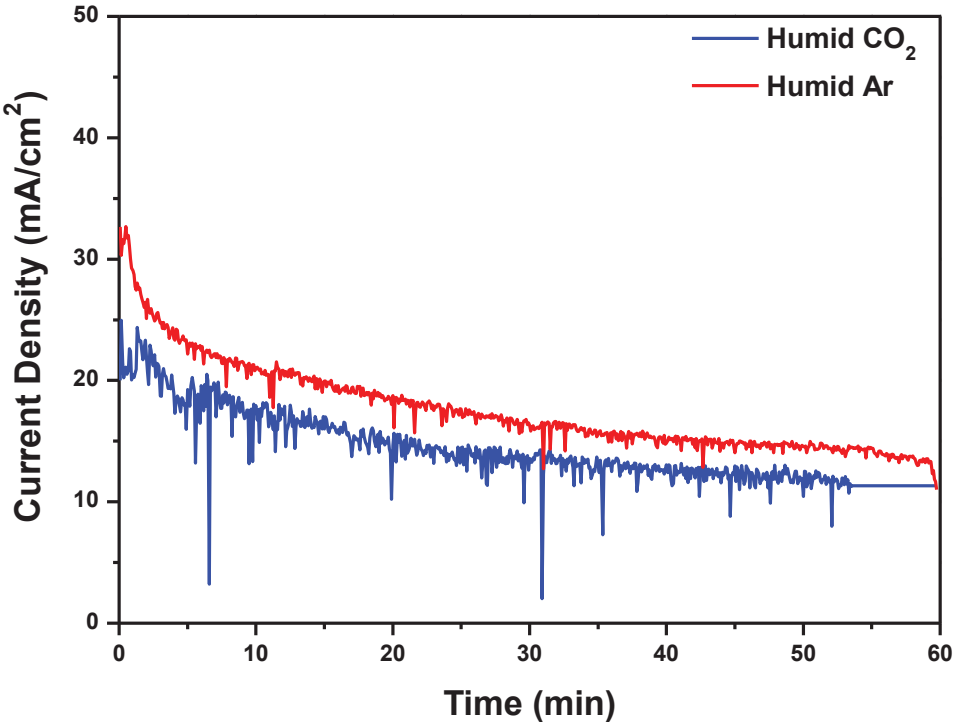

Fig. 3. Current-time curves resulting from electrolysis performed in molten chloride with and without CO_2 at 2V and 375 ºC in GFOE mode.

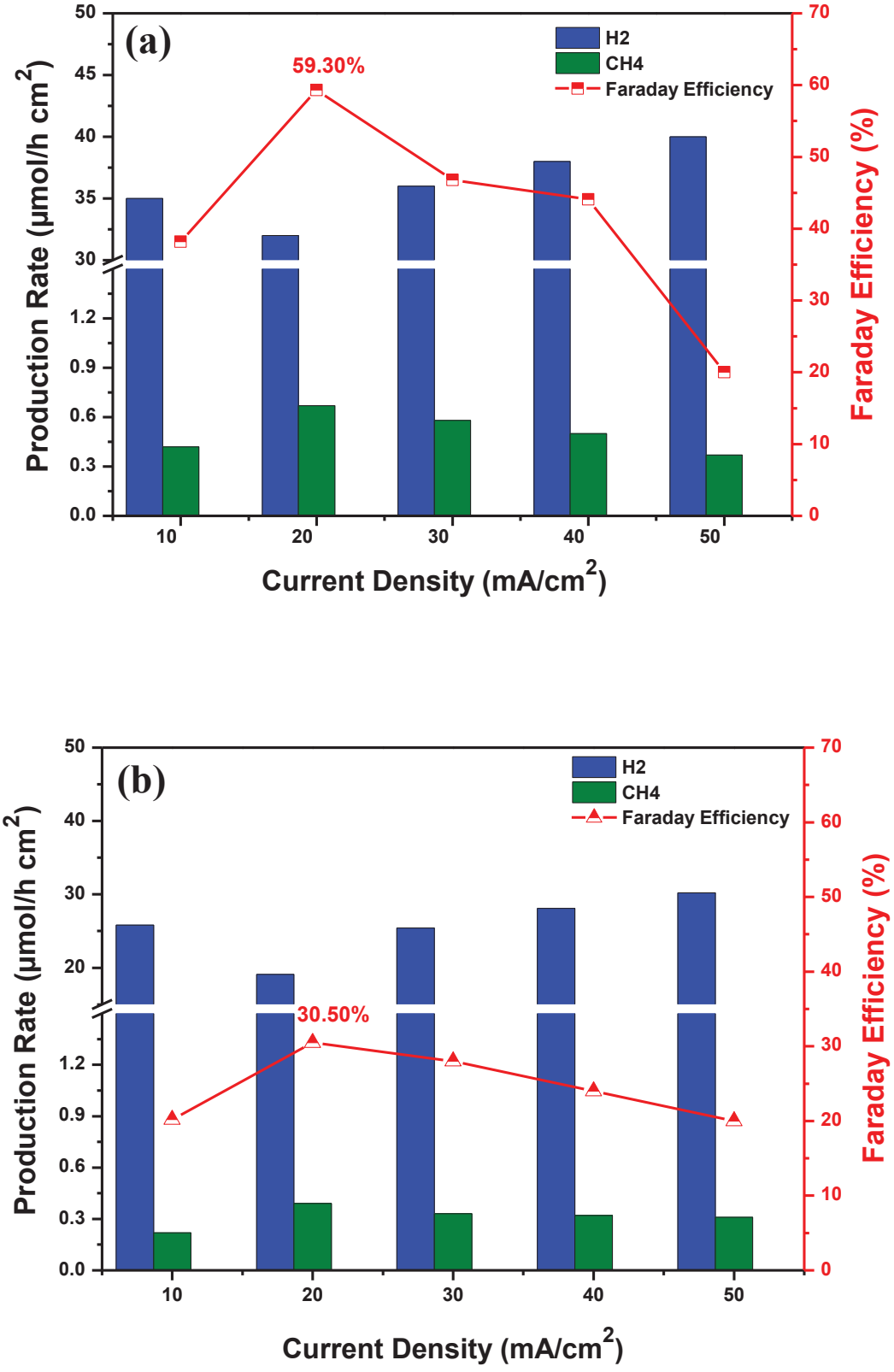

Fig. 4. The faraday efficiency and production rates of gaseous products at 2 V and 375 ºC under different current density in case of molten chloride electrolysis during GFIE mode after (a) 30 min (b) 60 min.

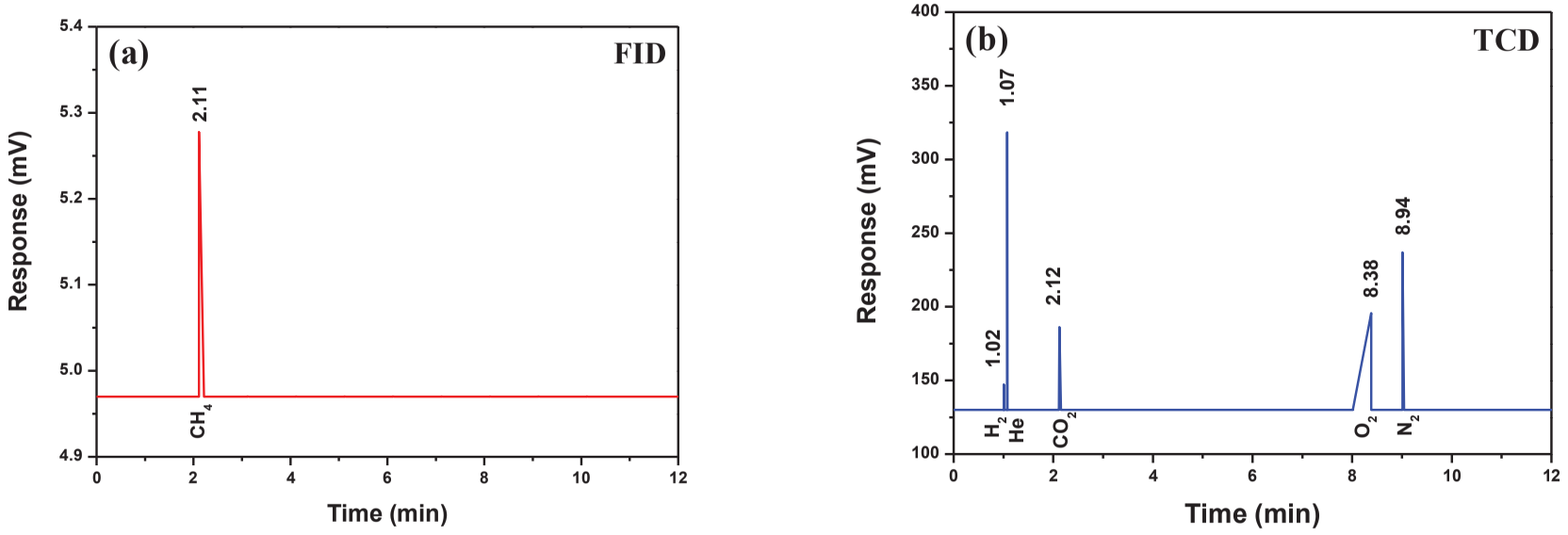

Fig. 5. The gas chromatography analysis of gaseous products in case of molten chloride electrolysis at 375 ºC and 2 V by (a) FID detector (b) TCD detector.

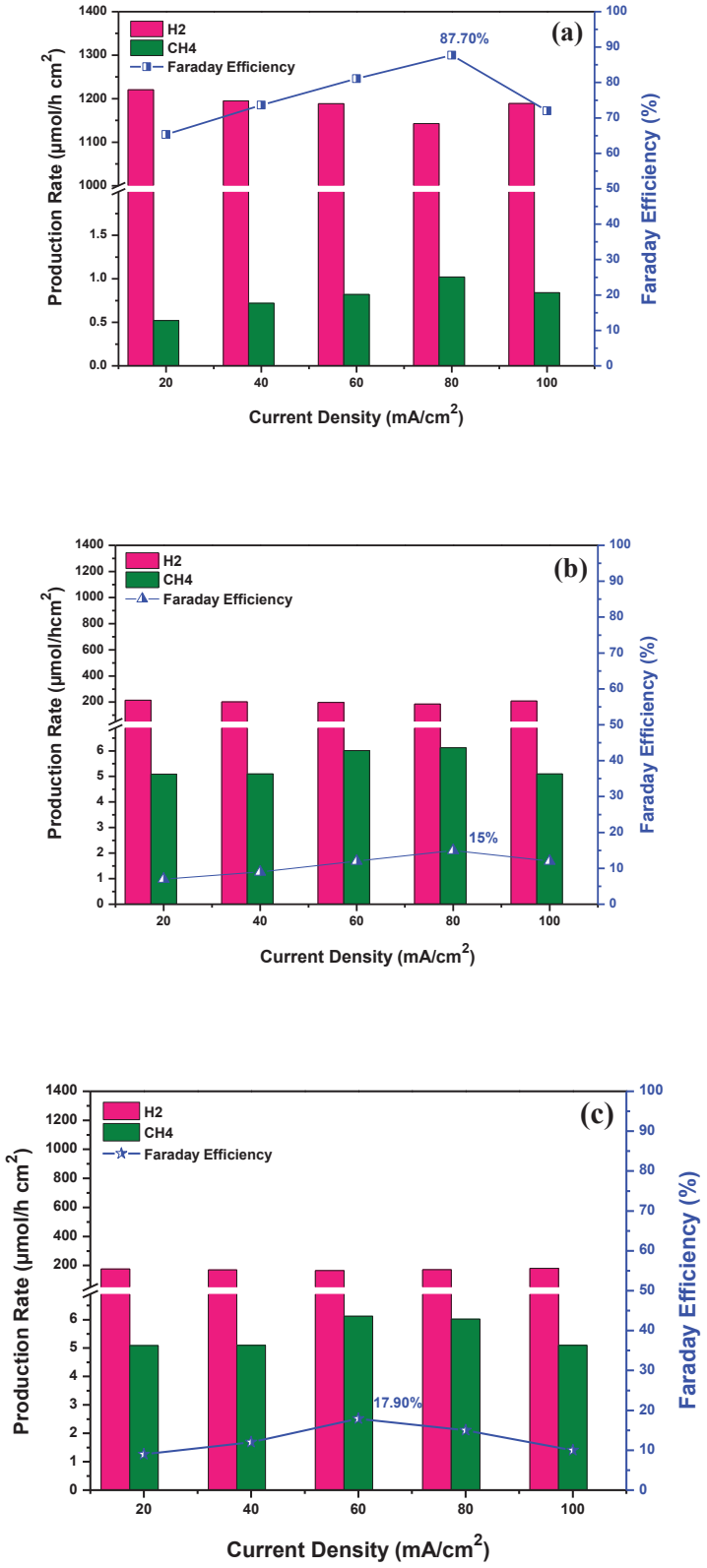

Fig. 6. The faraday efficiency and production rates of gaseous products at 2 V under different current density after electrolysis in; (a) LiOH-NaOH with GFOE mode at 275 ºC(b) LiOH-NaOH with GFIE mode at 275 ºC (c) KOH-NaOH with GFIE mode at 225ºC.

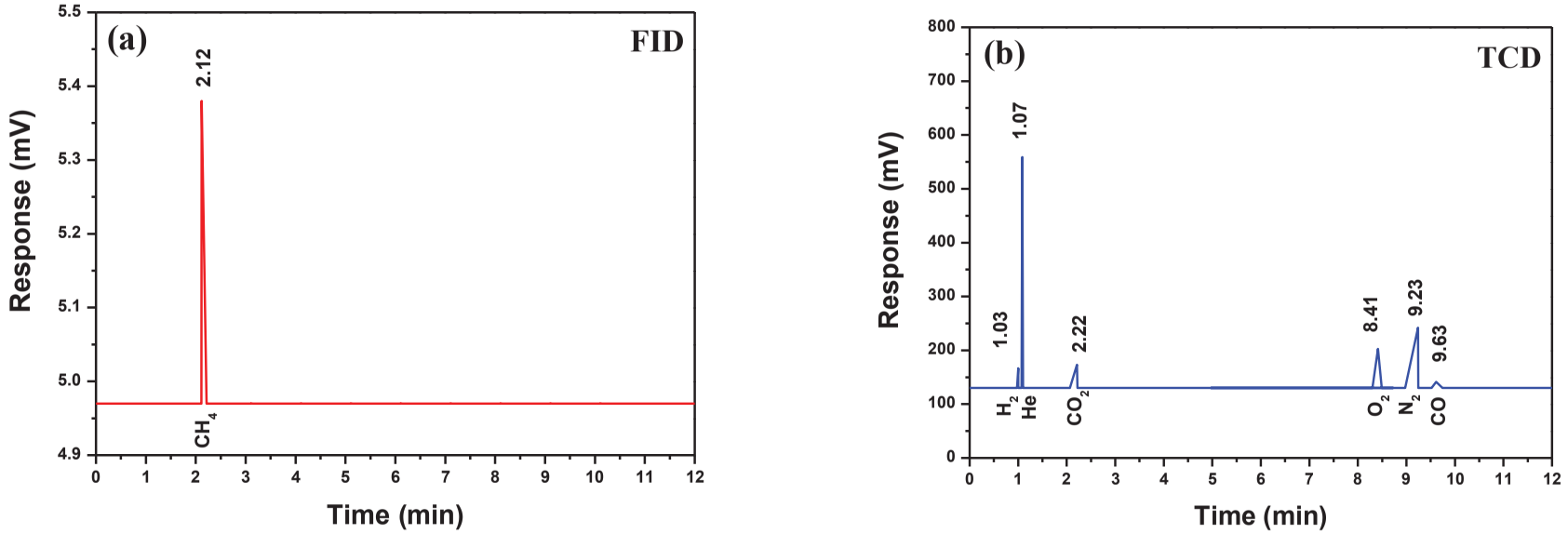

Fig. 7. The gas chromatography analysis of gaseous products in case of molten hydroxide (LiOH-NaOH) electrolysis by (a) FID detector (b) TCD detector.

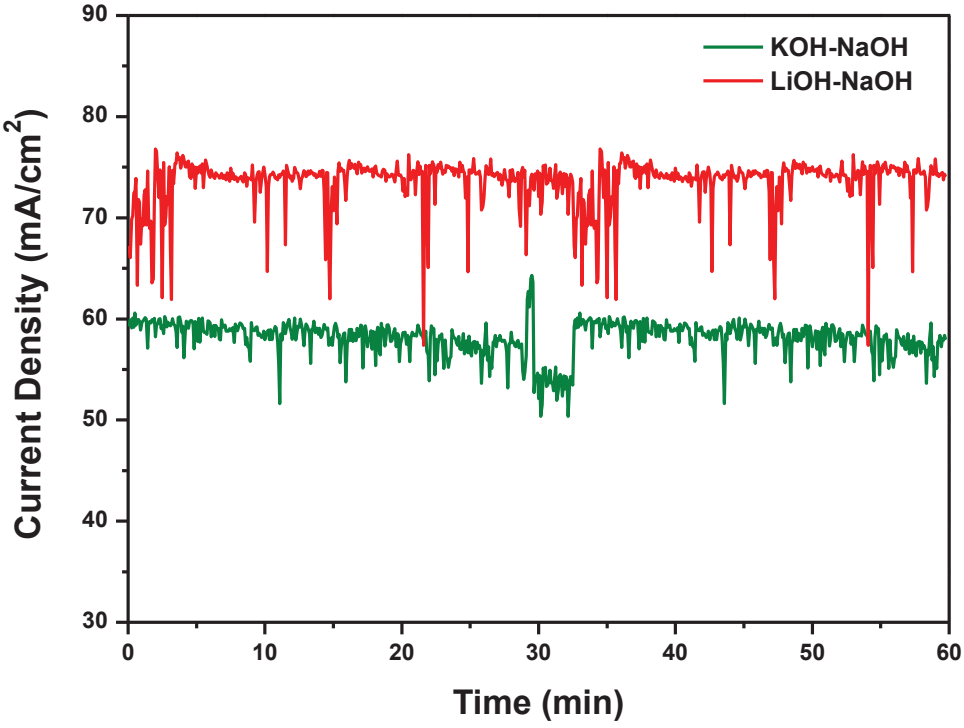

Fig. 8. Current-time curves resulting from electrolysis performed in two different molten hydroxides at 2V.

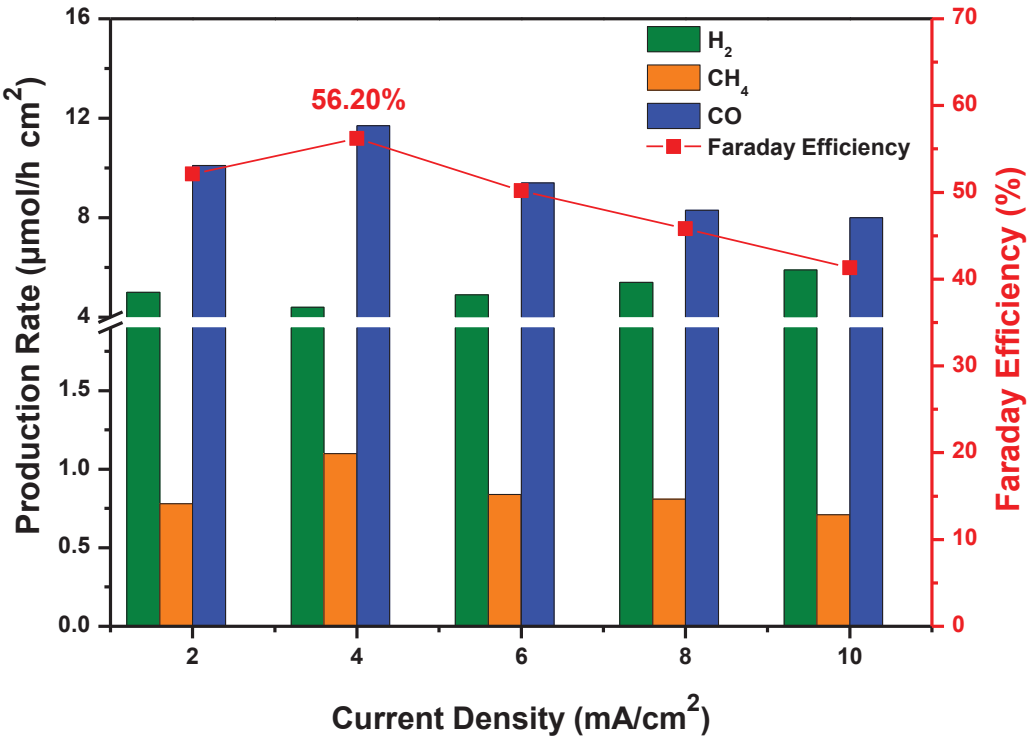

Fig. 9. The faraday efficiency and production rate of gaseous products at 1.5 V and 425 °C under different current density in molten carbonate electrolyte.

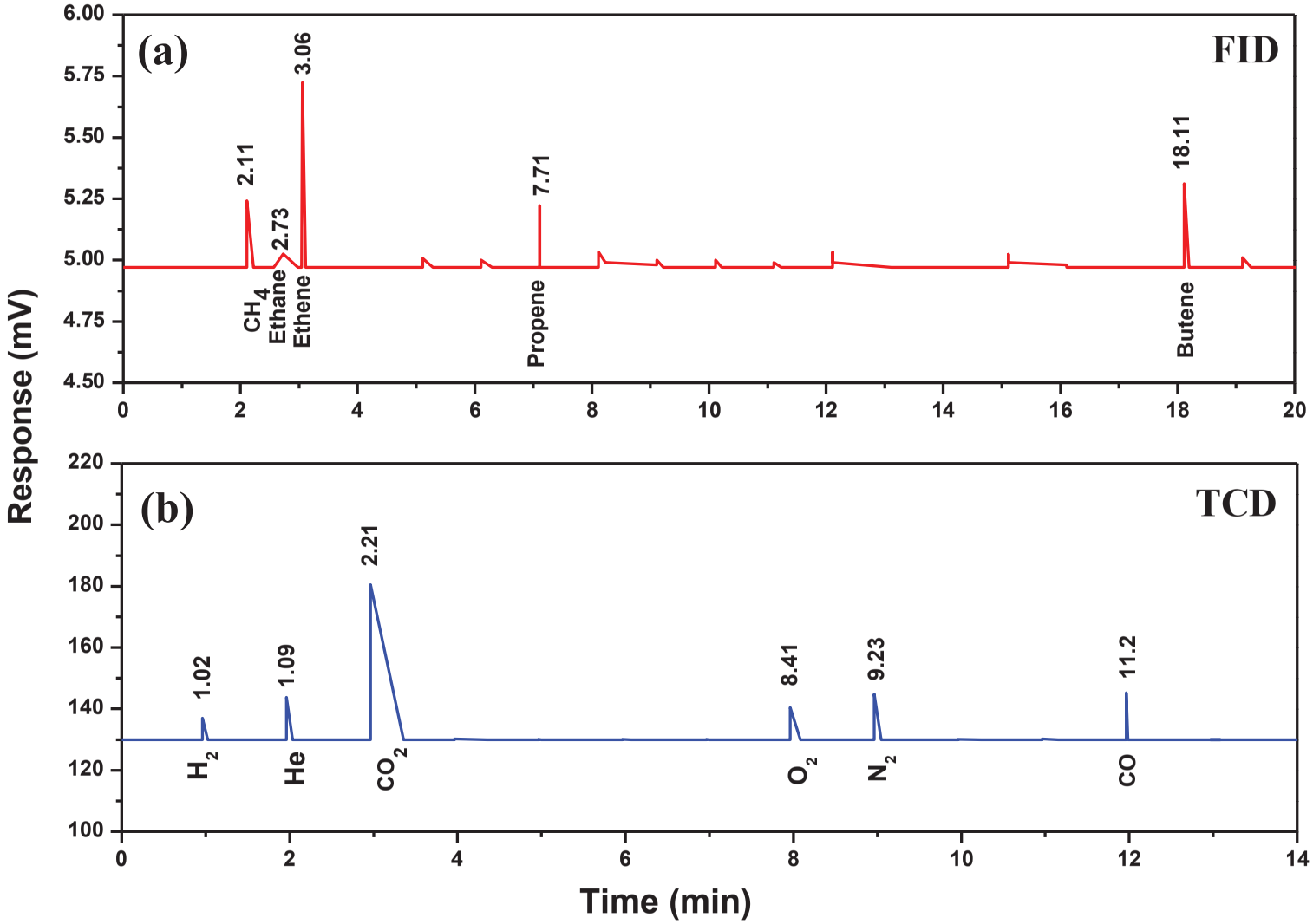

Fig. 10. The gas chromatography analysis of gaseous products in case of molten carbonate electrolysis by (a) FID detector (b) TCD detector.

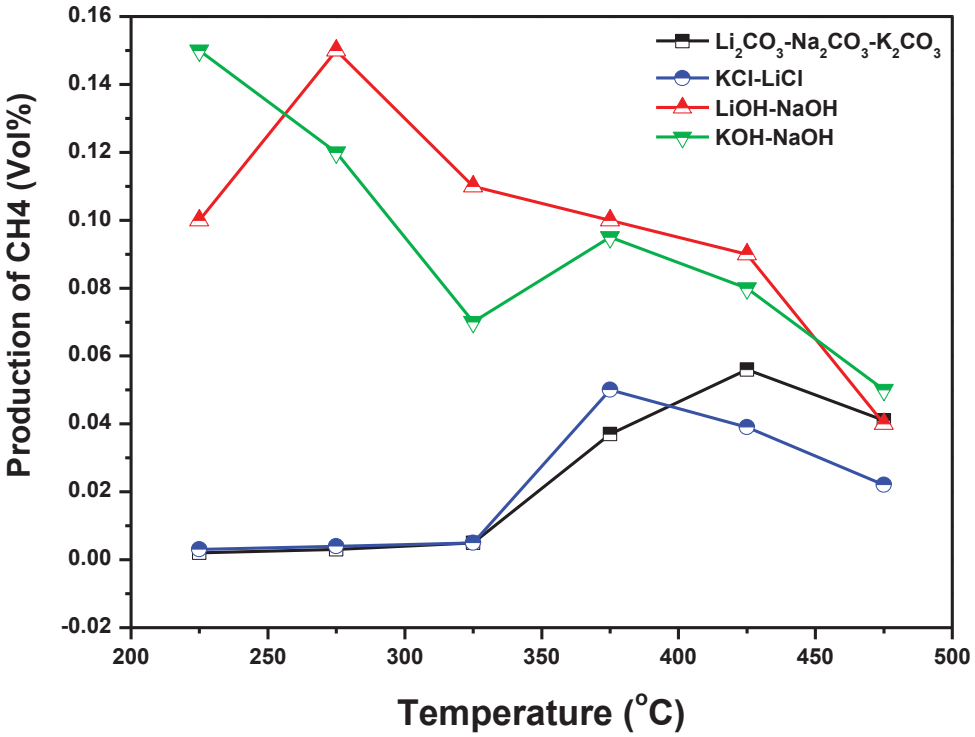

Fig. 11. The selection of optimum temperatures for all electrolytes on the basis of CH_4 production.

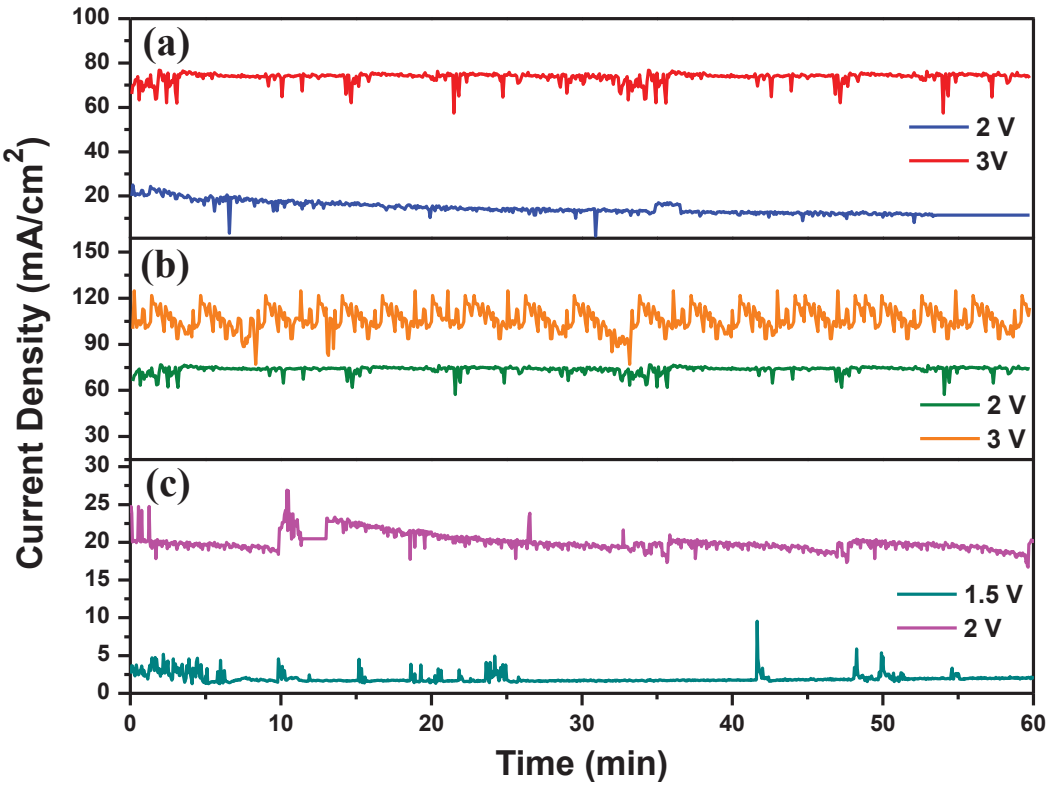

Fig. 12. The current density vs time plot at different voltages for three types of electrolytes; (a) molten chloride, (b) molten hydroxide and (c) molten carbonate.

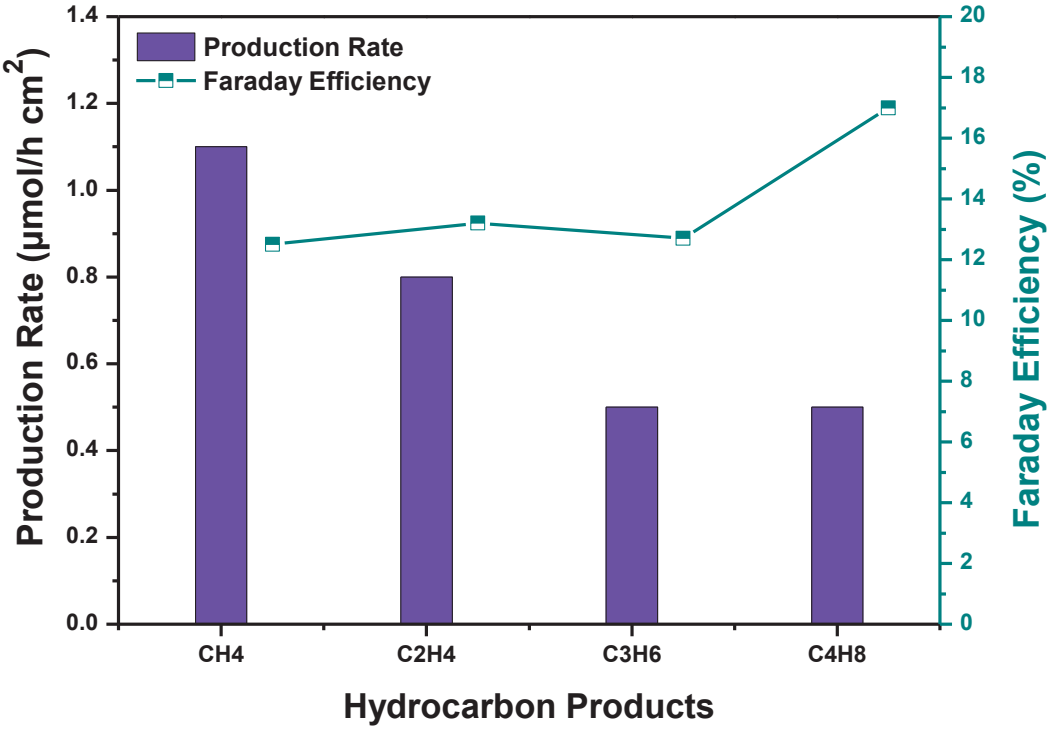

Fig. 13. The faraday efficiency and production rates of higher hydrocarbons at 1.5 V and 425 ^{o}C in case of molten carbonate electrolysis.

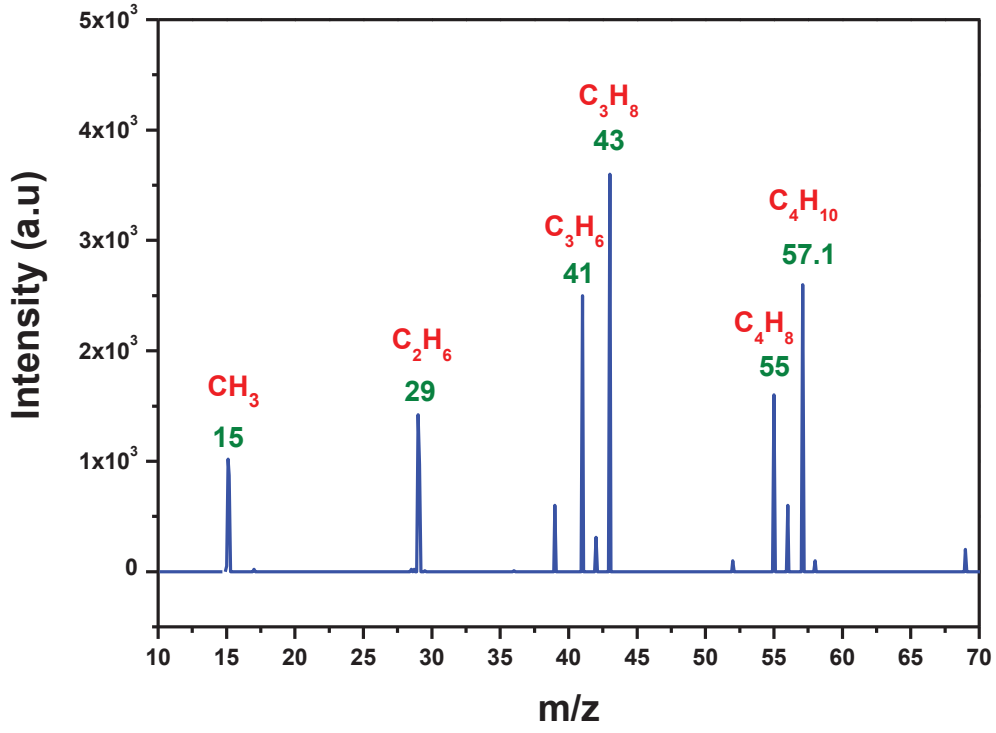

Fig. 14. The mass spectrum of compounds showing hydrocarbon after electrolysis in molten carbonate electrolyte under 1.5 V at 425 ℃.

List of Tables

Table 1.Specification of cathodic gas products in molten chloride salt with GFIE mode of electrolysis at 2V and 375 ^{o}C by using GC analysis.

Products	**Gas product composition (vol. %)**		**Uncertainty of gas composition**		**Faraday efficiency (%)**		**Energy consumption (J)**	
	(30 min)	(60 min)	(30 min)	(60 min)	(30 min)	(60 min)	(30 min)	(60 min)
H_2	2.40	2.48	±0.10	± 0.10	54.80	28.20	278.00	311.00
CH_4	0.05	0.05	±0.005	±0.005	4.50	2.30		
CO	0.00	0.00	0.00	0.00	0.00	0.00		
CO_2	34.80	4.84	–	–	–	–		
H_2O	2.00	2.00	–	–	–	–		
Ar	60.70	90.60	–	–	–	–		

Table 2. Specification of cathodic gas products during electrolysis in molten hydroxide (LiOH-NaOH) at 275 ºC and (KOH-NaOH) at 225 ºC under 2V applied voltage using GC analysis.

roducts	Gas product composition (vol. %)			Uncertainty of gas composition			Faraday efficiency (%)			Heating values (J)		Energy consumption (J)	
	*LiOH-NaOH	**LiOH-NaOH	**KOH-NaOH	*LiOH-NaOH	**LiOH-NaOH	**KOH-NaOH	*LiOH-NaOH	**LiOH-NaOH	**KOH-NaOH	**LiOH-NaOH	**KOH-NaOH	**LiOH-NaOH	**KOH-NaOH
H_2	27.3	4.44	3.94	± 0.90	± 0.10	± 0.10	87.30	13.00	15.60	130.00	116.00		
CH_4	0.03	0.15	0.15	± 0.004	± 0.01	± 0.01	0.40	2.00	2.30	14.00	12.00		
CO	0.00	0.00	0.00	0.00	0.00	0.00	0.00	0.00	0.00	0.00	0.00		
CO_2	0.480	0.750	0.580	–	–	–	–	–	–	–	–	1200.00	1000.00
H_2O	0.00	0.00	0.00	–	–	–	–	–	–	–	–		
Ar	72.20	94.70	95.30	–	–	–	–	–	–	–	–		

* After electrolysis with GFOE mode

** After electrolysis with GFIE mode

Table 3. Specification of cathodic gas products after electrolysis in molten carbonate at 1.5 V and 425 ºC by using GC and mass spectrometric analysis.

Product	Gas product composition (vol. %)	Uncertainty of gas composition	Faraday efficiency (%)	Heating value (J)	Energy consumption (J)
H_2	0.22	±0.04	11.90	11.40	
CH_4	0.06	±0.005	12.50	10.40	
C_2H_4	0.04	±0.003	13.20	12.00	
C_3H_6	0.03	±0.005	12.70	11.00	114.20
C_4H_8	0.03	±0.002	17.00	14.50	
CO	0.58	±0.09	31.80	35.30	
CO_2	52.70	–	–	–	
H_2O	2.40	–	–	–	
Ar	44.00	–	–	–	

Table 4. List of ΔG and ΔH for the generation of hydrocarbon products from the Fischer-Tropsch reaction (through CO_2 and water formation) and partial oxidation of methane at 425 ºC.

Products	Fischer-Tropsch Reaction				CH_4 partial oxidation	
	ΔG (kJ/mol)		ΔH (kJ/mol)		ΔG (kJ/mol)	ΔH (kJ/mol)
	CO_2 formed	H_2O formed	CO_2 formed	H_2O formed		
CH_4	-61.41	-48.37	-257.70	-220.10	–	–
C_2H_6	-52.03	-25.94	-445.90	-369.90	-138.20	-175.90
C_2H_4	-2.10	23.98	-303.40	-227.40	-297.20	-278.90
C_3H_8	-39.60	-0.47	-549.30	-435.30	-273.30	-267.10
C_3H_6	-5.69	33.44	-423.70	-309.70	-448.30	-387.00
C_4H_{10}	-43.31	8.86	-722.60	-570.60	-424.50	-428.10
C_4H_8	-18.62	33.55	-710.60	-558.70	-608.80	-661.70

For Table of Contents Use Only

The co-electrolysis of CO_2 and H_2O in molten chloride, molten hydroxides and molten carbonates was performed at moderate temperatures for sustainable hydrocarbons formation.